New Mexico Geological Society

Downloaded from: https://nmgs.nmt.edu/publications/guidebooks/50



PaleoProterozoic deformation, metamorphism, and $^{40}Ar/^{39}Ar$ thermal history of the 1.65 GA Manzanita Pluton, Manzanita Mountains, New Mexico

Cynthia L. Brown, Karl E. Karlstrom, Matthew Heizler, and Dan Unruh
1999, pp. 255-268. https://doi.org/10.56577/FFC-50.255

in:

Albuquerque Geology, Pazzaglia, F. J.; Lucas, S. G.; [eds.], New Mexico Geological Society 50 th Annual Fall Field Conference Guidebook, 448 p. https://doi.org/10.56577/FFC-50

This is one of many related papers that were included in the 1999 NMGS Fall Field Conference Guidebook.

Annual NMGS Fall Field Conference Guidebooks

Every fall since 1950, the New Mexico Geological Society (NMGS) has held an annual Fall Field Conference that explores some region of New Mexico (or surrounding states). Always well attended, these conferences provide a guidebook to participants. Besides detailed road logs, the guidebooks contain many well written, edited, and peer-reviewed geoscience papers. These books have set the national standard for geologic guidebooks and are an essential geologic reference for anyone working in or around New Mexico.

Free Downloads

NMGS has decided to make peer-reviewed papers from our Fall Field Conference guidebooks available for free download. This is in keeping with our mission of promoting interest, research, and cooperation regarding geology in New Mexico. However, guidebook sales represent a significant proportion of our operating budget. Therefore, only *research papers* are available for download. *Road logs*, *mini-papers*, and other selected content are available only in print for recent guidebooks.

Copyright Information

Publications of the New Mexico Geological Society, printed and electronic, are protected by the copyright laws of the United States. No material from the NMGS website, or printed and electronic publications, may be reprinted or redistributed without NMGS permission. Contact us for permission to reprint portions of any of our publications.

One printed copy of any materials from the NMGS website or our print and electronic publications may be made for individual use without our permission. Teachers and students may make unlimited copies for educational use. Any other use of these materials requires explicit permission.

This page is intentionally left blank to maintain order of facing pages.

PALEOPROTEROZOIC DEFORMATION, METAMORPHISM, AND $^{40}AR/^{39}AR$ THERMAL HISTORY OF THE 1.65-GA MANZANITA PLUTON, MANZANITA MOUNTAINS, NEW MEXICO

CYNTHIA L. BROWN[1], KARL E. KARLSTROM[1], MATTHEW HEIZLER[2], and DAN UNRUH[3]
[1]Department of Earth and Planetary Sciences, University of New Mexico, Albuquerque, NM 87131; [2]New Mexico Bureau of Mines and Mineral Resources, 801 Leroy Place, Socorro, NM 87801; [3]U.S. Geological Survey, Federal Center, Denver, CO 80225

Abstract—The 1.65-Ga Manzanita pluton and its aureole record an interaction of Paleoproterozoic plutonism, deformation, and metamorphism in New Mexico. Field observations and microscopic analysis indicate that the pluton was emplaced during regional NW–SE shortening. Synchronous plutonism and contact metamorphism are indicated by an increase in temperature from regional metamorphic greenschist grade rocks to contact metamorphic amphibolite grade rocks. Peak contact metamorphic temperatures and pressures of 600–620°C and 2–3 kbar are shown by assemblages with Fe-rich andalusite + K-feldspar + biotite + quartz + white mica + oxides. Synchronous deformation and metamorphism is indicated by contact metamorphic mineral-matrix relationships including the growth of garnet before, during, and after development of the regional S_2 foliation, sillimanite that is both randomly oriented and aligned along S_2, and hornblende that is dynamically recrystallized along S_2. Synchronous plutonism and regional deformation is indicated by parallel magmatic and solid-state fabrics, dynamic recrystallization of feldspar indicating high-T solid-state deformation, variably deformed dikes and veins that cross-cut, and are also folded by, regional foliation, and dike orientations consistent with a regional kinematic framework of NW–SE shortening. New radiometric dates constrain the timing of synpluton tectonism. The Manzanita pluton has been dated by U-Pb-zircon techniques at 1645 ± 16 Ma. In addition, a post-S_2 rhyolite dike to the south of the pluton cooled through 300°C at 1428 ± 2.0 Ma, determined through $^{40}Ar/^{39}Ar$ techniques. Hornblende in the contact aureole of the pluton yields variable $^{40}Ar/^{39}Ar$ ages of circa 1.4 Ga and 1.67 Ga, interpreted as hornblende growth at 1.65 Ga and reheating at 1.4 Ga to 400–500°C.

INTRODUCTION

The nature and timing of plutonism, deformation, and metamorphism in Proterozoic rocks in New Mexico are complex and have been a topic of debate. In one model, tectonism was considered to be mainly early Proterozoic (ca. 1.65 Ga), and ascribed to the formation of continental lithosphere through the accretion of arc terranes, with synchronous plutonism, deformation, and prograde metamorphism (Karlstrom and Bowring, 1988; Bowring and Karlstrom, 1990; Bauer and Williams, 1994). In another model, metamorphism was considered middle Proterozoic (ca. 1.4 Ga), synchronous with regional deformation and emplacement of voluminous granitic plutons in the middle crust (Grambling et al., 1988; Grambling and Dallmeyer, 1993; Ralser et al., 1997; Marcoline et al., 1999).

Recent research has focused on the recognition of the importance of both 1.65 Ga and 1.4 Ga tectonism (Thompson et al., 1996; Karlstrom et al., 1997; Pedrick et al., 1998; Williams et al., 1999). Nevertheless, the relationship and relative importance of these two events remains controversial for many regions. In any given location, it can be difficult to determine the relative importance of each event in producing the observed polyphase metamorphic assemblages and tectonic fabrics. Recent workers have documented aureole deformation and metamorphism synchronous with emplacement of 1.4-Ga plutons over a wide region (Nyman et al., 1994; Duebendorfer and Christensen, 1995; Kirby et al., 1995a; Thompson et al., 1996; Gonzales et al., 1996; Andronicos, et al., in prepartion). There are also areas where 1.4-Ga metamorphism and deformation occur in areas with no exposed 1.4-Ga plutons (Pedrick et al., 1998; Read et al., 1999; Williams et al., 1999). In these areas, the 1.4 Ga, high-grade metamorphic mineral assemblages are often difficult to distinguish from high-grade metamorphic assemblages interpreted to have grown in aureoles of the nearby 1.65-Ga plutons (Pedrick et al.,1998; Read, et al., 1999; Williams et al., 1999). This has made it difficult to tie confidently the deformation and metamorphism directly to the 1.65-Ga plutons. In each of these cases, regional metamorphic minerals such as monazite, sphene, garnet, and staurolite yield U-Pb dates of 1470–1420 Ma (Williams et al., 1999) and hornblende yields $^{40}Ar/^{39}Ar$ dates of 1420–1350 Ma (Karlstrom et al., 1997). Some workers have used these dates to suggest that all amphibolite metamorphism in New Mexico was 1.4 Ga, with older metamorphism and deformation at greenschist grade occurring at 1.65 Ga (Marcoline et al., 1999). Others have argued that hornblende grew at 1.65 Ga, and the 1.4 Ga dates represent a resetting due to loss of Ar during regional reheating and localized deformation at 1.4 Ga (Bauer and Williams, 1994). One test of these alternatives is to examine areas where the 1.65 Ga event is believed to have been higher grade than the 1.4-Ga overprint. Karlstrom et al. (1997) showed that the Sandia-Manzano Mountains at 1.4 Ga were probably initially cooler, and also cooled more quickly, than areas in northern New Mexico. Thus, the Sandia-Manzano uplift is an ideal place to examine 1.65-Ga metamorphism and deformation.

The Manzanita pluton of the Sandia-Manzano uplift (Fig. 1) has been dated at 1645 Ma ±16 Ma (see below). It shows a narrow amphibolite grade contact aureole on its south margin grading to regional greenschist grade metamorphism away from the pluton. Because any single piece of geologic evidence for relative timing relationships can be spurious (Paterson and Tobisch, 1988), we present multiple lines of evidence that together link synchronous contact metamorphism and deformation and synchronous deformation and plutonism. Combining these independent arguments, the goal of this paper is to show that amphibolite-grade contact metamorphism was synchronous with regional deformation and pluton emplacement at 1.65 Ga, with deformation continuing during and after pluton cooling. Later deformation and metamorphism at 1.4 Ga was a less intense overprinting of the earlier dominant event.

GEOLOGIC BACKGROUND

The Manzanita Mountains in central New Mexico are part of a Proterozoic orogenic belt that extends cross-strike from Wyoming to Chihuahua, Mexico. The region is part of the Mazatzal Province, an area interpreted to record a major pulse of continental assembly during the Mazatzal orogeny of 1.70–1.60 Ga. U-Pb zircon dates on volcanogenic rocks of the Mazatzal province in New Mexico range from about 1680 to 1660 Ma (Bowring and Karlstrom, 1990; Bauer et al., 1993; Bauer and Williams, 1994). The Proterozoic rocks in the Manzanita Mountains are exposed in a narrow uplift that is bounded on the west by Tertiary age normal faults and associated sediments related to the Rio Grande rift, and on the east by unconformably overlying

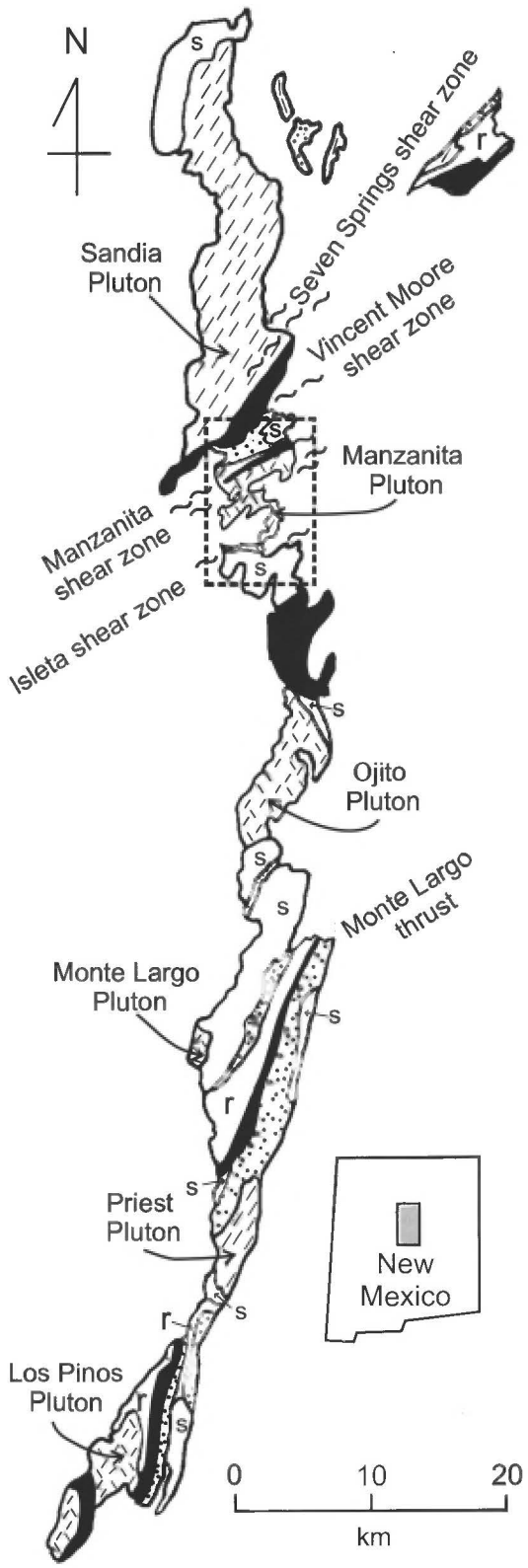


FIGURE 1. Simplified geologic map of the Sandia, Manzanita, Manzano, and Los Pinos Mountains thrust belt (after Karlstrom et al., 1997). Dashed box shows location of area of study that is shown in Figure 2. Inset shows location of thrust belt in New Mexico. Rock units are as follows: dashed lines = 1.4 Ga granites, showing magmatic fabric; cross-hatched = 1.65 Ga granites; white with s = schist and phyllite, including lithic arenite, Coyote schist, and Blue Springs schist; dotted = quartzite, including Sais, White Ridge, and Cerro Pelon; white with r = metarhyolite, including Sevilleta metarhyolite; black = metavolcanics, amphibolite and mafic schist.

Paleozoic strata (Reiche, 1949; Myers and McKay, 1970). Recent work (Chamberlin et al., 1997) has shown that the Manzanitas are part of a ductile thrust belt that extends 115 km from the Sandia Mountains in the north to the Los Pinos Mountains in the south (Fig. 1).

Lithologies

Manzanita pluton

The main unit of the Manzanita pluton is a strongly deformed, homogenous, pink, quartz monzonite (Chamberlin et al., 1997) with 1–4-cm K-feldspar phenocrysts (now porphyroclasts). A less voluminous unit, present only at the north and south margins, is a weakly to moderately deformed, orange, two-mica, medium-grained, non-porphyritic quartz monzonite (Chamberlain et al., 1997). The units are interpreted to represent separate, yet coeval or continuous, intrusive events, as shown by the lack of crosscutting relationships and the presence of gradational contacts in the north. Leucocratic granite, aplite, and pegmatite dikes occur throughout the Manzanita pluton and its margins, and are interpreted to represent evolved phases of the Manzanita pluton.

Supracrustal rocks

Metasedimentary and metavolcanic supracrustal rocks are on the north and south margins of the pluton (Fig. 2). The supracrustal rocks are probably equivalent to rocks dated at 1680 Ma in the southern Manzano Mountains (Bauer et al., 1993). The base of the section is a metavolcanic unit, composed of heterogeneous basaltic greenstones, intermediate volcanics including dacite tuff and breccia, volcaniclastic greenschists, and metapelites interfingered with buff schistose bands and andesitic volcanic rocks. The metavolcanic unit is overlain by a lithic arenite interbedded with, and overlain by, a blue-gray phyllite, a pure massive quartzite, and a quartz-rich schist (Brown, 1999).

Regional structural fabrics

Three foliations are recognized in the mapped area. The earliest tectonic fabric, S_1, is visible microscopically in samples from areas to the north and south of the Manzanita pluton. It is defined by aligned metamorphic minerals in microlithons and porphyroblasts (Fig. 3A) and fold noses (Fig. 3B) that are folded by F_2 folds (sample locations are circles 1 and 2, respectively, on Fig. 2). Cavin (1985) also noted the fabric (also his S_1) north of the pluton as an early foliation that was defined by micas and transposed into the dominant foliation (also his S_2), but Parchman (1981) did not note this earlier fabric. Both S_1 and S_2 foliations could have formed during a single progressive shortening event, here called the D_2 event. S_1 and S_2 fabrics may have developed at about the same regional metamorphic grade as shown by the growth of biotite during the development of both fabrics (Fig. 3A).

The dominant tectonic fabric in the area, S_2, corresponds to a regional penetrative foliation that strikes northeast to east-northeast and dips approximately 45° SE. A stretching lineation, defined by elongated minerals, rakes steeply on foliation planes. A top-to-the-northwest shear sense was determined in the field and microscopically (Brown, 1999) through observations of shear sense indicators, including shear band cleavages (also know as C-type and C'-type cleavages and C/S fabrics), mantled porphyroclasts and porphyroblasts, strain shadows, mica and oxide fish, and the vergence of asymmetric fold sections (Simpson and Schmidt, 1983; Passchier and Trouw, 1996). All thin sections used for determination of shear sense were cut parallel to the stretching lineation and perpendicular to the foliation (see Figs. 3, 4, 14 for examples of shear sense). Although the fabric is present across the entire Manzanita pluton and in areas to the north and south, areas of more intense shearing bound the pluton. Many of these areas were described as discrete thrust faults by earlier workers (Parchman, 1981; Cavin, 1985), but we interpret them to be shear zones because of their ductile character and gradational relationship with thrust-sense shear fabrics throughout the area.

A variably developed crenulation cleavage, S_3, is present in country

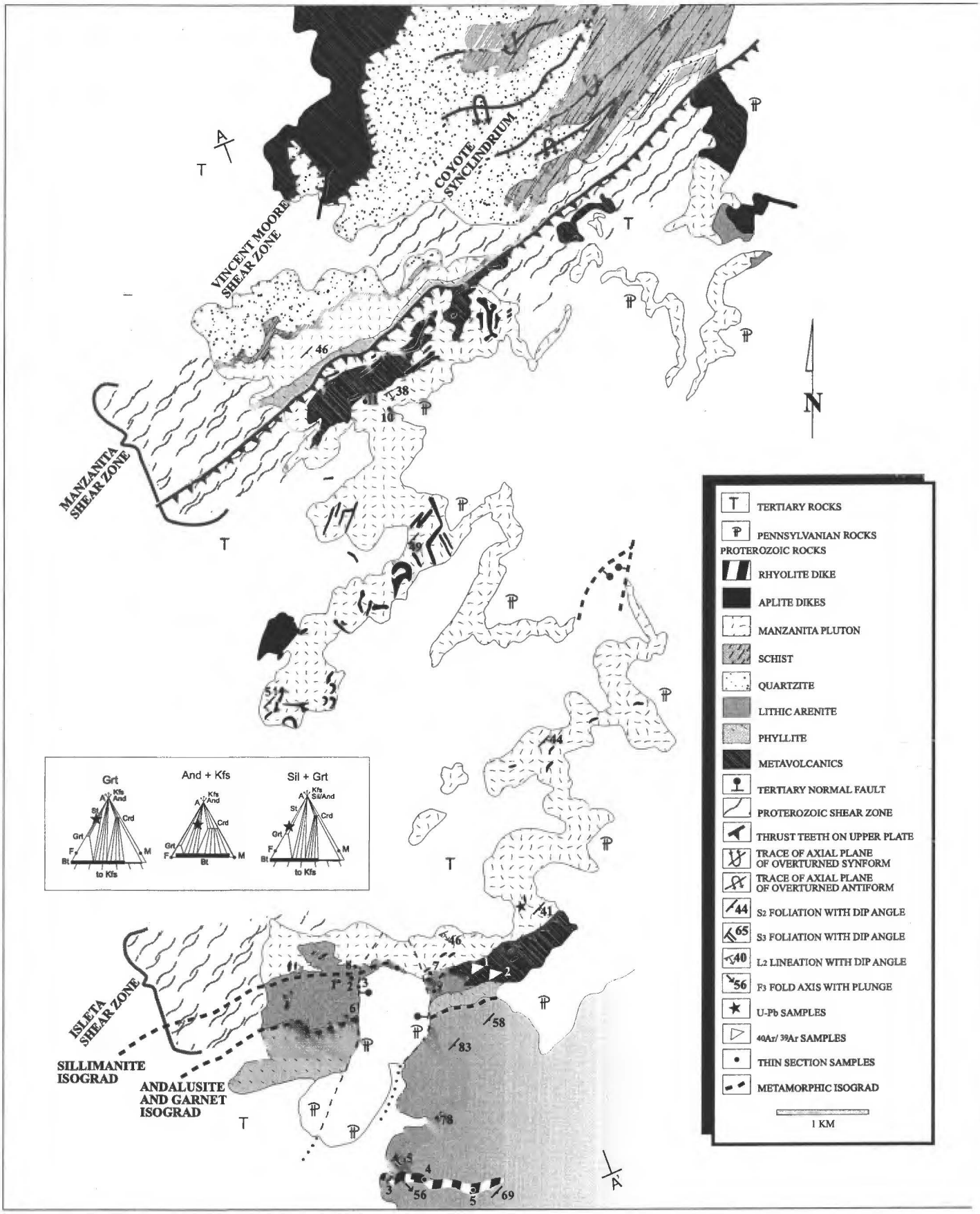


FIGURE 2. Geologic map of the Manzanita pluton and surrounding Proterozoic rocks, showing generalized rock type, metamorphic isograds, and sample locations (discussed in text). Marks with A and A' show location of simplified cross section in Figure 15A. Inset shows AFM diagrams for selected assemblages (see text).

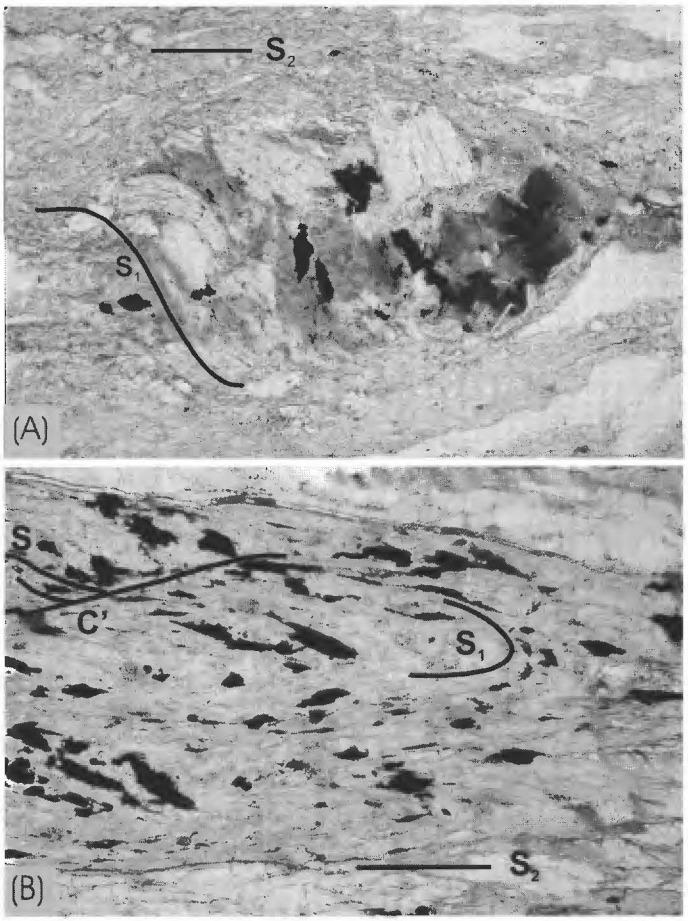


FIGURE 3. Photomicrographs of metamorphic minerals showing S_1. **A**, Biotite with opaque inclusions perpendicular to S_2. Note the muscovite grain included in the upper left of the biotite that is bent into the S_2 foliation. Note top-to-the-left (north) shear sense. **B**, White mica with opaque inclusions showing noses of F_2 folds. Note S-C fabric in upper left showing top-to-the-left (north) shear sense. Sample locations are shown on Figure 2 as circles 1 and 2, respectively. Width of view is 2.1 mm for both.

rocks on the north and south margins of the pluton. The axial planar cleavage strikes variably northeast to southeast and is subvertical; F_3 fold axes plunge southeast.

Major structures and map features

The following section describes the major structures and map features in a north-to-south transect shown in Figure 2. Primary structures in supracrustal rocks are rarely preserved, but there are sufficient cross-beds, pillow structures, and graded beds to help document the facing of map-scale folds and unit sequences to the north and south (Fig. 2). The Vincent Moore shear zone to the north (named the Vincent Moore thrust by Cavin, 1985) is a low-angle, 1–10-m-wide shear zone with greenschist-grade phyllites, schists, and quartzites in the upper plate (Andronicos et al., in prepartion). The quartzites and schists south of the Vincent Moore shear zone, and north of the Manzanita pluton, are folded in an asymmetrical, north-verging, upward-facing, southwest-plunging synclinorium with an axial plane parallel to S_2 (Cavin, 1985). The folds in the synclinorium are structurally overlain by thrust sense shear zones as part of the 2–4-km-wide Manzanita shear zone (new name).

The Manzanita granite is intimately associated with the Manzanita shear zone. This zone includes the Coyote "thrust" of Cavin (1985), but is a wide zone of more intense shearing, rather than a single thrust. The zone is characterized by a complexly interfingered contact zone between the Manzanita granite and country rock, including sections of greenstone and phyllonite (formerly phyllite) completely contained within the granite. The Manzanita shear zone shows a significant reduction in grain size; the granite grades from a porphyroclastic augen gneiss outside of the zone to an impressive array of mylonite and ultramylonite textures within the zone. The ultramylonite was interpreted to be metarhyolite by Cavin (1985), but is interpreted here to be mylonitic Manzanita Granite based on preserved K-feldspar porphyroclasts similar in size to K-feldspar phenocrysts in the Manzanita Granite.

The Isleta shear zone is a wide shear zone on the south margin of the Manzanita pluton that includes the Isleta thrust of Parchman (1981) and the contact zone between the Manzanita Granite and country rock. The western two-thirds exposure of the Isleta shear zone is characterized by a complex interfingering of granite and country rock with many screens and mylonitic fabrics (Fig. 4; see circle 3 on Fig. 2 for sample location), whereas the eastern exposure is a discrete, straight thrust fault with no screens. Two km south of the Isleta shear zone is a porphyritic rhyolite dike intruding concordant with S_2. The dike shows no evidence of S_2-associated deformation, but does show some mild S_3-associated deformation (Fig. 5; see circles 4 and 5 on Fig. 2 for sample locations). Farther to the south in Hell Canyon are a synclinorium and anticlinorium with axial planes parallel to S_2 (Parchman, 1981; Chamberlin et al., 1997).

GEOCHRONOLOGY

U-Pb analytical procedures

Zircon was separated from the Manzanita Granite (see star on Fig. 2 for sample location) using conventional heavy-liquid and magnetic separation techniques. Zircons, chosen to yield samples free from inclusions and as clear as possible, were spiked with a ^{205}Pb, ^{233}U, and ^{236}U-enriched tracer and were dissolved in HF in a vapor-transfer bomb (Krogh, 1978). Samples were then directly loaded on single Re-filaments with phosphoric acid and silica gel. Lead was run as the element and U as the oxide, UO_{2+}, using a VG Sector 54, 7-collector solid-source mass spectrometer. The Pb blank for the procedure was 10–20 pg (10^{-12} g) and that for U was <1 pg.

U-Pb results and discussion

Eleven single-crystal samples and one multi-crystal sample from NM91 were analyzed for U and Pb concentrations and Pb isotopic compositions. Data are shown in the Appendix and are plotted on a U-Pb concordia diagram (Fig. 6). The data define a linear array that intersects the concordia diagram at 1645 ± 16 Ma and 37 ± 39 Ma (95% C.I., Ludwig, 1985). The upper intercept is interpreted to represent the emplacement age of the granite, whereas the lower intercept probably has no rigorous age significance. The lower intercept reflects compara-

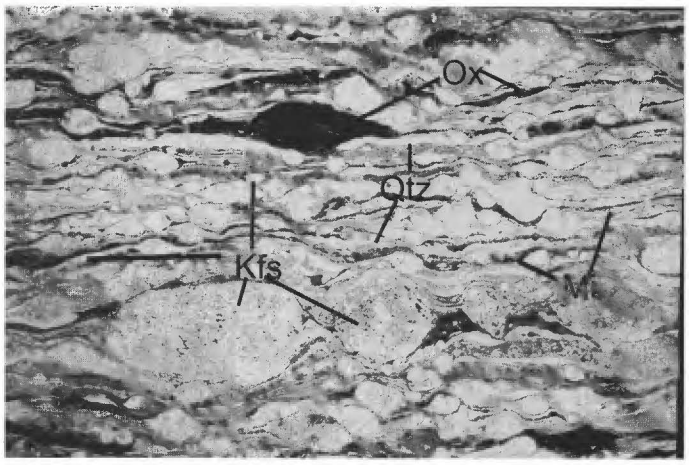


FIGURE 4. Photomicrograph of Manzanita granite from the Isleta shear zone, showing typical mylonite fabric and top-to-the-left (north) shear sense. Note rounded grain-sized reduced feldspar grains (Kfs), with a relict larger grain in the lower left, and ribbons of quartz (Qtz), mica (Mi), and oxides (Ox). Width of view is 17 mm. Sample location is shown on Figure 2 as circle 3.

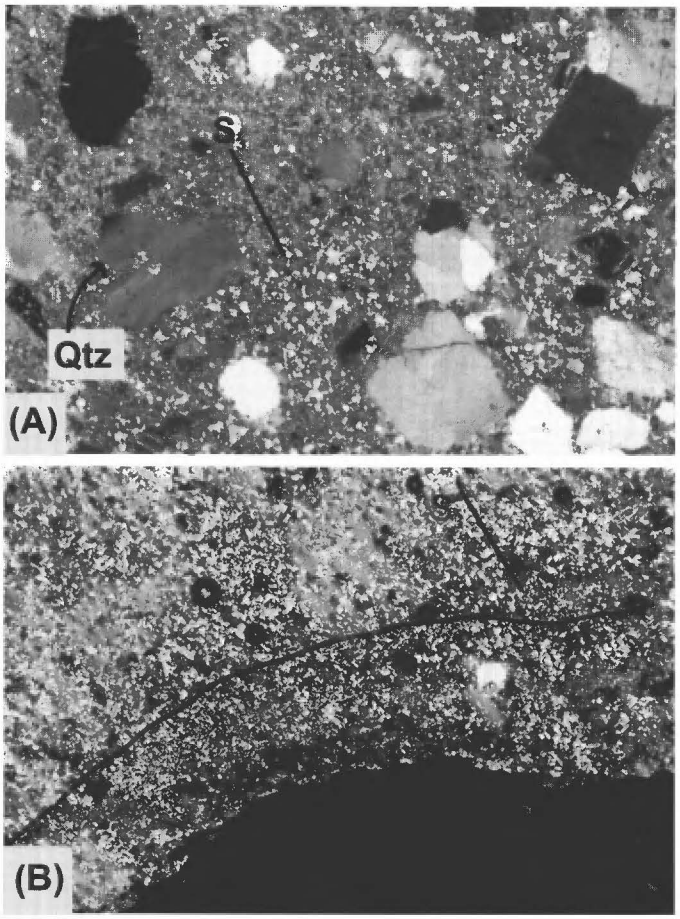


FIGURE 5. **A**, Photomicrograph of sample from the interior of the rhyolite dike showing volcanic, euhedral phenocrysts 5–8 mm across, including embayed quartz grain (arrow), set in a fine grained matrix. Deformation is mild with some quartz grains showing undulatory extinction and micas slightly aligned in S_3. Width of view is 0.82 mm. Sample is courtesy Matt Nyman. **B**, Photomicrograph of sample from the chilled dike margin showing magmatic flow textures (curved line) parallel to the margin and crenulated by S_3. Micas are oriented along S_3. The alignment of micas and margin crenulation along S_3, combined with the total lack of S_2-associated deformation indicates that the dike was emplaced after S_2 development and before or during S_3 development. Width of view is 2.1 mm. Sample locations are shown on Figure 2 as circles 4 and 5, respectively.

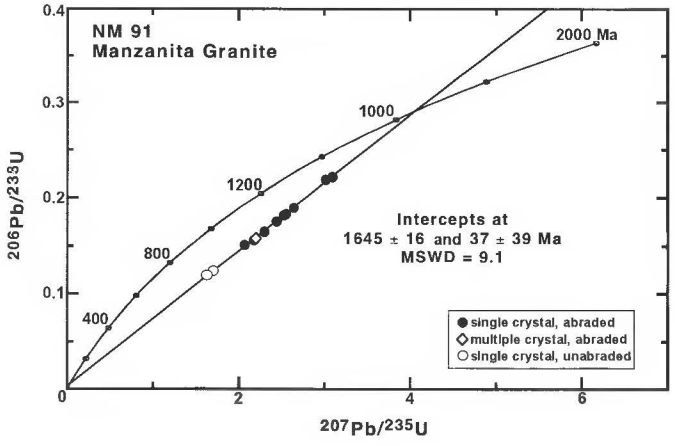


FIGURE 6. Uranium-lead data for sample NM91 (see star on Fig. 2 for sample location). Uncertainties are smaller than the size of the symbols. The data, though discordant, define an apparent age of 1645 ± 16 Ma.

tively recent Pb loss, perhaps during uplift of the area with effects of recent weathering superimposed.

The 16-Ma uncertainty in the emplacement age is somewhat larger than would normally be expected for a pluton of this age. The larger uncertainty is both a function of the discordance of the data points and the amount of scatter about the best-fit line. Although the data for the abraded samples are much more concordant than from the unabraded samples, these data are still 20–40% discordant. The degree of discordance of the individual points correlates with the U content and by inference the amount of radiation damage to the crystal lattices.

The data also exhibit significant excess scatter about the best-fit line as exemplified by the MSWD = 9.1. The rather high MSWD is typical of discordant data and may reflect multiple recent episodes of Pb loss as mentioned above, or may reflect minor disturbances to the U-Pb systems of the zircons induced during metamorphism at ~1.4 Ga. Given this latter possibility as well as the discordant nature of the data, we view the 1645 ± 16-Ma date as a minimum age for pluton emplacement.

$^{40}Ar/^{39}Ar$ analytical procedures

Three hornblende samples from the metavolcanic unit (KMW-12, KMW-13, and K96-1; see triangles 1, 1, and 2, respectively, on Fig. 2 for sample locations) and one muscovite sample from the rhyolite dike (NM-109; see triangle 3 on Fig. 2 for sample location) were analyzed by the $^{40}Ar/^{39}Ar$ incremental heating method. Analytical procedures and detailed isotopic results may be found in Heizler (1998).

$^{40}Ar/^{39}Ar$ results and discussion

The KMW-12 and KMW-13 spectra are complex and yield overall saddle-shaped release patterns while the K96-1 spectrum is essentially flat yielding a plateau age of 1432.1 ± 4.7 Ma (Fig. 7A). The initial 30% of the muscovite spectrum shows decreasing ages followed by a flat segment (plateau age = 1428.0 ± 2.0 Ma) for the final 70% of ^{39}Ar released (Fig. 7B). The isochron array for sample KMW-13 reveals significant scatter (MSWD = 72), but the data appear to indicate excess argon contamination (cf. Heizler and Harrison, 1988) and provide an intercept age of 1651 ± 42 Ma. Isochron data for the remaining samples are exceptionally clustered due to nearly identical and high (~99%) radiogenic yields and therefore are not shown.

Despite the high degree of scatter for the isochron array from KMW-13, we suggest that the sample may have a cooling age of 1651 ± 42 Ma and note that this age is indistinguishable from the crystallization age of 1645 ± 16 Ma determined for the Manzanita pluton. Considering the geographic proximity of the hornblende samples it may be difficult to understand how one sample was reset at ca. 1.4 Ga while the others were not. It is possible that all of the samples are truly 1.4 Ga and are simply contaminated with excess argon. We do not prefer this interpretation because the isochron for KMW-13 is more consistent with a 1.65-Ga cooling age rather than a 1.4-Ga resetting age. There are many factors that presumably control the argon retentivity of amphiboles. Both experimental and field based studies reveal variable retentivity depending upon parameters such as composition, exsolution, mineral structure, grain size, and alteration (Harrison, 1981; Harrison and Fitz Gerald, 1986; Onstott and Peacock, 1987; Cosca and O'nions, 1994; Dahl, 1996; Villa et al., 1996). Because the protolith for the amphibole-bearing rocks is a heterogeneous metavolcanic unit, there is considerable variability in bulk composition, as well as the degree of deformation observed.

METAMORPHISM

Rocks in and around the Manzanita pluton preserve evidence of at least three "phases" of metamorphism: (1) regional greenschist grade metamorphism to the north and south of the pluton, which is interpreted to represent peak conditions at 1.65 Ga and 1.4 Ga; (2) contact metamorphism around the Manzanita pluton, which is interpreted to be the age of the pluton (1.65 Ga); and (3) retrograde metamorphism in the pluton and the country rocks to the north and south, which may record the retrograde path during and after the cooling of the pluton, as well as

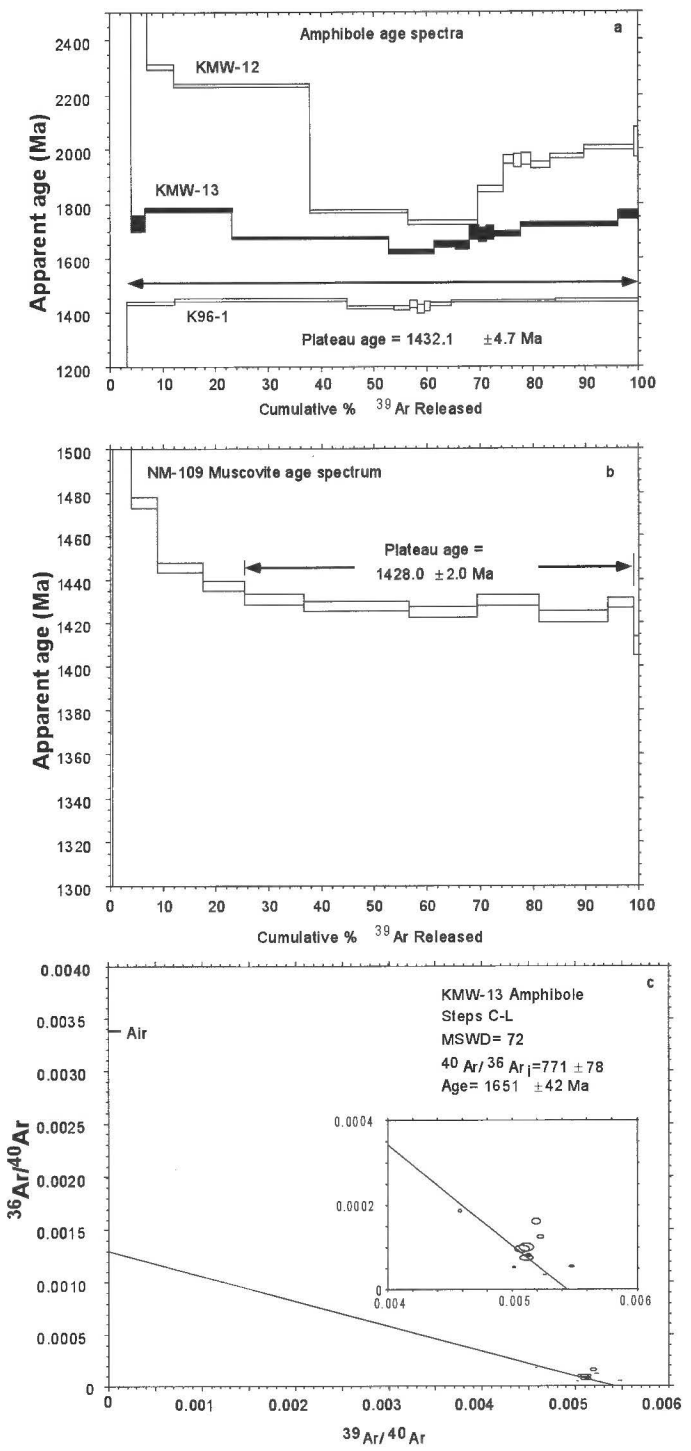


FIGURE 7. **a** and **b**, Age spectra for amphiboles and mica. **c**, Isochron plot for KMW-13 amphibole. See triangles 1, 1, and 2 on Figure 2, respectively, for sample locations. See Figure 11 for photomicrograph of sample KMW-13.

cooling at 1.4 Ga. Table 1 presents data for key assemblages; for a complete list of thin sections analyzed and their assemblages, see Brown (1999).

Regional metamorphism

Regional metamorphism north to the Vincent Moore shear zone and south to the Hell Canyon area (Fig. 1) is middle to upper greenschist facies, with typical assemblages in metabasaltic rocks of albite +/- actinolite + epidote/clinozoisite + chlorite + oxides +/- quartz +/- white mica (Parchman, 1981; Cavin, 1985; this study). Microprobe and optical data indicate that plagioclase in these rocks is <An8 in composition to the south (Parchman, 1981) and <An4 to the north (Cavin, 1985). The presence of actinolite with epidote and albite indicates temperatures below 500°C (Miyashiro, 1994; Laird and Albee, 1981; Apted and Liou, 1983). Some samples to the south may contain small amounts of hornblende together with actinolite, indicating that temperatures approached 500°C, although it cannot be determined if this occurred in the Paleoproterozoic or the Mesoproterozoic. Parchman (1981) suggested that the presence of hornblende may be due to heating from nearby dikes. Still farther to the south, just north of the Ojito pluton, greenstones contain hornblende, not actinolite, but the hornblende is probably related to contact aureole effects around the Ojito pluton (Edwards, 1978).

A typical metasedimentary assemblage to the south of the Manzanita pluton is white mica + chlorite + biotite + quartz (Parchman, 1981; this study), and may represent the reaction:

$$\text{chlorite} + \text{K-feldspar} = \text{muscovite} + \text{biotite} + \text{quartz} + H_2O$$

This reaction marks the first appearance of biotite and muscovite together in the same rock, and probably occurs between 300°C and 400°C (Spear, 1993). Another typical assemblage to the south is albite + white mica + chlorite + quartz; the white mica may include pyrophyllite, which is not easily distinguished optically, and probably represents a higher-Al bulk composition at temperatures of <400°C (Spear and Cheney, 1989).

To the north of the Manzanita pluton, a typical regional metapelitic assemblage is white mica + quartz + chlorite (Cavin, 1985; this study) and again, probably represents temperatures of less than 400°C. Farther to the north, just above the Vincent Moore shear zone, quartzites contain white mica + quartz ± boudinaged kyanite altered to a low-relief, low-birefringent mineral that is possibly cordierite (Brown, 1999). Andronicos et al. (in press) and Kirby et al. (1995b) suggest that these rocks crystallized between 380°C and 500°C with pressure greater than 2.5 kbar. Kyanite + quartz is also found in pre-1.4-Ga regional conditions away from the Priest pluton (Fig. 1) and as inclusions inside contact metamorphic andalusite in the Priest pluton aureole (Thompson et al., 1996) and in this study area (see below), suggesting that the upper greenschist assemblage may represent regional conditions throughout the Manzanita and Manzano Mountains.

The presence of margarite + quartz + chloritoid + chlorite in at least one sample analyzed by microprobe (Cavin, 1985), indicates temperatures of between 300°C and 560°C and pressures of <8.6 kbar, but the reaction is somewhat pressure dependent (Chatterjee, 1976). Based on pressures from the south of the pluton, the pressure here is most likely <3 kbar, which further restricts the temperature to be <450°C (Chatterjee, 1976). Chloritoid has only been found north of the Manzanita pluton (Parchman, 1981; Cavin, 1985; this study) and may also have grown due to heat from the pluton, but there are presently not enough data to determine its extent.

Contact metamorphism at 1.65 Ga

Contact metamorphism around the Manzanita pluton is demonstrated by a sharp increase in grade towards the pluton, represented in pelitic rocks on the south margin (Fig. 2). A contact aureole has not been observed on the north margin of the Manzanita pluton. Because there has been intense retrogression including sericitization of many minerals close to the pluton margins, it is difficult to determine the exact location of isograds. The location of isograds representing a particular pressure and temperature may also be affected by subtle changes in bulk composition, particularly in Fe content. Parchman (1981) shows the garnet—in isograd and the andalusite—in isograd. Our distribution of assemblages shows the presence of garnet and andalusite at similar distances from the pluton, and we therefore designate only one isograd to represent both index minerals, the garnet/andalusite isograd. In addition, the sillimanite isograd is located closer to the pluton (Fig. 2).

Garnet appears within approximately 650 m (this study; see Fig. 2) to

TABLE 1. List of key assemblages and their geographic distribution and points of interest.

Rock Type	Typical Assemblage	Geographic Distribution	Key Points of Interest
Lithic Arenite	White mica, chlorite, biotite, quartz, oxides	South of Manzanita pluton (outside contact aureole) to Hell Canyon and one small area on pluton's north margin	Regional greenschist-grade metamorphism
	Sillimanite, garnet, plagioclase, quartz, white mica, chlorite (retrograde), oxides	One sample just south of Manzanita pluton in contact aureole	Peak contact metamorphism; sillimanite is syn-S_2. T = 600–650°C, P = 2–3 kbar
	Andalusite, K-feldspar, biotite, quartz, white mica, oxides	Manzanita pluton contact aureole on south margin	Peak contact metamorphism; T = 600–620°C, P = 2–3 kbar
	Garnet, andalusite, white mica quartz, oxides	Manzanita pluton contact aureole on south margin	Contact metamorphism; garnet is syn-S_2. T = 575–610°C, P = 2–3 kbar
Metavolcanics	Chloritoid, margarite, chlorite, quartz, oxides	Found north of Manzanita pluton in pelitic ayers; extent of distribution not well established	Probably represents regional metamorphism; chloritoid shows retrogression syn-S_2. T = 300–560°, P <8.6 kba
	Actinolite, albite, epidote/ clinozoisite, chlorite, quartz, white mica, oxides	North and south of Manzanita pluton (outside contact aureole)	Regional greenschist-grade metamorphism; T <500°C
	Hornblende, plagioclase, quartz, epidote, oxides	Manzanita pluton contact aureole on south margin	Contact metamorphism; T >500°C
Quartzite	Kyanite, cordierite(?), quartz, white mica, plagioclase, chloritoid(?)	Hanging wall of the Vincent Moore shear zone north of Manzanita pluton	Regional metamorphism; T 380–500°, P >2.5 kbar

1 km (Parchman, 1981) from the pluton. The garnet is not associated with either biotite, chloritoid, or staurolite in any samples, but typically occurs with andalusite (often with pink cores indicating higher Fe content). Garnet may have formed via:

$$\text{Fe-staurolite} + \text{quartz} = \text{almandine} + Al_2SiO_5 + H_2O$$

The garnets are generally less than 0.5 mm, and no inclusions of staurolite could be optically resolved, but the lack of biotite combined with the presence of andalusite indicates this to be the most likely garnet-forming reaction and infers that the garnet is Fe-rich (see inset on Fig. 2 for garnet AFM diagram). The presence of almandine + andalusite indicates temperatures were 500–580°C or higher (Spear, 1993, p. 344, 361). Based on an estimated pressure of about 2–3 kbar (see below), the temperature was 575–610°C (Spear, 1993).

Rocks containing the assemblage andalusite + K-feldspar + quartz + white mica + biotite + oxides ± chlorite (retrograde) ± plagioclase are present within 650 m from the pluton (see inset on Fig. 2 for andalusite + K-feldspar AFM diagram). The presence of K-feldspar in equilibrium with andalusite (Fig. 8; see circle 6 on Fig. 2 for sample location) indicates the reaction:

$$\text{muscovite} + \text{quartz} = \text{andalusite} + \text{K-feldspar} + H_2O$$

This reaction is supported by the common presence of inclusions of white mica within andalusite. Samples with andalusite and K-feldspar also contain white mica and quartz, which would indicate the assemblage is univariant. The andalusite has a high-Fe content, however, as indicated by pale pink pleochroic cores with anomalous extinction. The Fe content adds a degree of freedom, thus stabilizing the four-phase assemblage across a wider P-T interval. Grambling and Williams (1985) linked similar optical properties in andalusite in north-central New Mexico to Fe and Mn contents and recalculated the reaction curves for Fe-containing Al_2SiO_5. The andalusite in this study has anomalous extinction ranging from brown (corresponding to 0.05– 0.08 atoms Mn + Fe per 5 oxygens; Grambling and Williams, 1985) to bright blue (corresponding to 0.09–0.12 atoms Mn + Fe^{3+}; Grambling and Williams, 1985); the extra component is probably all Fe, because the cores display only pink, and not green, pleochroism (Grambling and Williams, 1985).

The presence of andalusite + K-feldspar restricts the P-T field to less than about 2 kbar, and 550–700°C (Spear, 1993). The position of the muscovite-out reaction moves to the left with increasing Fe content, however, based on a decreased activity of andalusite, but the movement of the curve is affected by the partitioning of Fe into andalusite and muscovite. The Fe in andalusite could have come from oxides or muscovite; because the Fe content of muscovite in these samples is unknown, it is difficult to accurately calculate the position of the muscovite-out reaction curve. The position of the muscovite-out reaction curve could also be affected by water activity, where $P_{H2O} < P_{total}$ would also shift the reaction curve to the left (Kerrick, 1972; Spear, 1993, p. 322–326). In the absence of graphite or carbonates, which further reduce the H_2O content of the rocks, we estimate $P_{H2O} = 0.8$. Based on a likely minimum pressure of 2 kbar, we interpret the peak T and P in the pluton aureole to be 600–620°C and 2–3 kbar.

Sillimanite was observed in only one sample, collected from an area directly adjacent to the pluton. It is fibrous and located inside a porphyroblast replaced by white mica that may also contain relict andalusite (Fig. 9; see circle 7 on Fig. 2 for sample location). There are numerous white mica porphyroblasts near the pluton, usually with relict

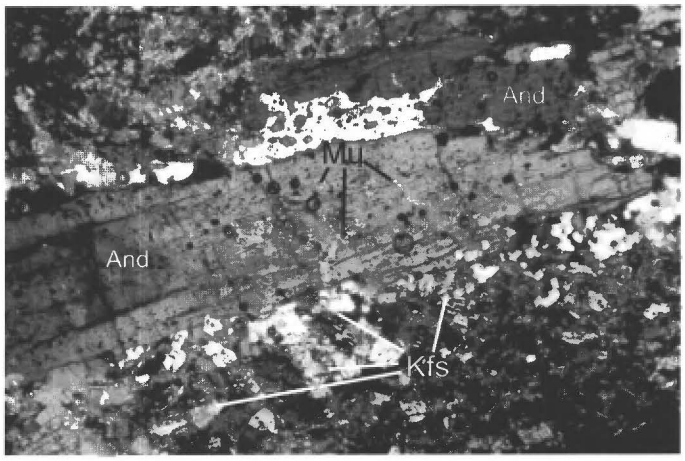


FIGURE 8. Photomicrograph of andalusite lath (And; possibly pseudomorphed after kyanite) and K-feldspar (Kfs) in equilibrium. Note white mica inclusions (Mu) in the andalusite. Width of view is 4.8 mm. Sample location is shown on Figure 2 as circle 6.

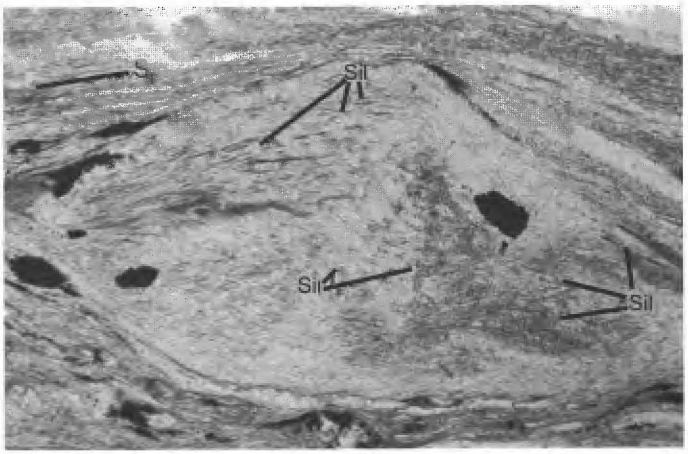


FIGURE 9. Photomicrograph showing fibrolitic sillimanite (Sil) in a white mica pseudomorph after an unknown porphyroblast (possibly andalusite). The sillimanite in the upper left and far right close to the edge of the porphyroblast is aligned subparallel to S_2, whereas the sillimanite in the lower right towards the interior is randomly oriented. Width of view is 2.1 mm. Sample location is shown on Figure 2 as circle 7.

grains of low birefringence that cannot be optically resolved but may be andalusite. The sillimanite is in a rock with the assemblage garnet, chlorite (retrograde), plagioclase, and white mica (see inset on Fig. 2 for sillimanite AFM diagram). Because andalusite is absent or mostly consumed in this rock, the sillimanite probably grew from the reaction:

andalusite = sillimanite

Based on the proximity to the pluton, this reaction probably represents an increase in temperature to perhaps 620–650°C. Alternatively, the sample may be from rocks with Fe-poor bulk composition, and the sillimanite could have grown at the same temperatures of 600–620°C as the andalusite + K-feldspar-containing rocks, and we therefore use these as peak conditions.

Textural relationships suggest the former presence of kyanite and hence either higher pressures or lower temperatures, or both, before pluton emplacement. In several samples the andalusite (in textural equilibrium with K-feldspar) displays a bladed habit typical of kyanite (Fig. 8), and in many other samples where the andalusite is poikilitic, the andalusite grains are optically oriented in a "ghost" grain with bladed habit. The bladed habit suggests that andalusite nucleated on the kyanite and grew by epitaxial growth and replacement (Kerrick, 1990). In one sample kyanite is preserved as embayed inclusions in andalusite (Fig. 10; also noted by Parchman, 1981).

Amphibole-bearing samples collected up to 300 m from the pluton on the south margin contain hornblende + epidote (retrograde?) + plagioclase + chlorite (retrograde?) ± quartz ± biotite. Although one sample near the pluton contains actinolite and not hornblende, there is a clear gradation from generally hornblende-bearing rocks close to the pluton to generally actinolite-bearing rocks away from the pluton, suggesting that hornblende grew during pluton emplacement. Hornblende in this study is typically characterized by a complex growth history; many grains have actinolite cores, and in some cases there appears to be a narrow rim of later hornblende, marked by a ring of opaques just inside the outer rim (Fig. 11; see triangle 1 on Fig. 2 for sample location). The presence of hornblende rather than actinolite generally represents T >500°C for common assemblages (Laird and Albee, 1981).

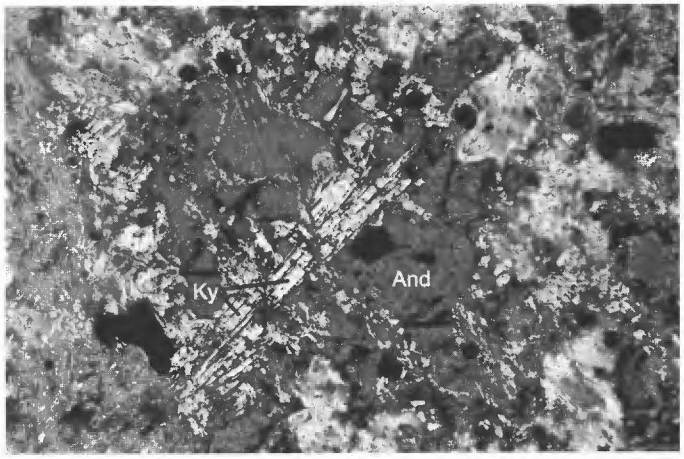


FIGURE 10. Photomicrograph of andalusite (And) with embayed kyanite (Ky). Width of view is 0.82 mm. Thin section is courtesy Mark Parchman.

Retrogression

Retrogression is present across the entire pluton and in the margins. Porphyroblasts in pelitic units and porphyroclasts of feldspar in the granite have been seriticized, and have often been completely replaced. In many cases, the reactions require water, indicating the presence of fluids during retrogression. On the north margin, where the retrogression is particularly intense, chloritoid has reacted to skeletons of hematite and is often boudinaged, with chlorite in the gaps and as beards aligned in S_2 (Brown, 1999). This suggests retrogression at approximately 350°C by the reaction after Thompson and Norton (1968):

2 chloritoid + 5 magnetite + 2 quartz + 4 H_2O = chlorite + 5 hematite

Along the south margin, euhedral, hexagonal porphyroblasts of undeformed quartz, white mica, and hematite with pressure shadows of opaques and chlorite, are possibly pseudomorphs after garnet (Brown, 1999), and may indicate the oxidizing reaction:

garnet + biotite + $^3/_2$ O_2 = 3 hematite + white mica + 3 quartz

The pluton also appears to be retrogressed throughout. Feldspars typically contain substantial amounts of sericite, sometimes being completely obscured. Laird and Albee (1981) and Miyashiro (1994) indicate that in low pressure areas, such as in contact metamorphism, the peristerite jump from albite to oligoclase is at lower temperatures than the growth of hornblende. Plagioclase throughout the pluton, as well as in most samples with hornblende from the south margin, was measured optically to contain An8 or less (Parchman, 1981; Cavin, 1985; this study). We interpret these An contents to indicate that retrogression in plagioclase has occurred throughout the Manzanita pluton and on its

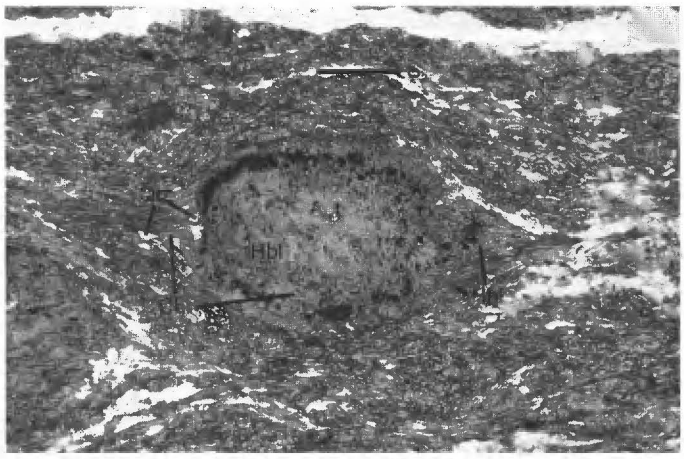


FIGURE 11. Photomicrograph of hornblende porphyroblast (Hbl) with core of actinolite (Act) and rim of opaques just inside the outer edge, showing typical complexity of amphiboles in the area. Porphyroblast has recrystallized hornblende, quartz (Qtz), and chlorite (Chl) in the tails that are sheared into S_2. Width of view is 2.1 mm. Sample location is shown as triangle 1 on Figure 2. This sample is KMW-13; see Geochronology section for discussion of $^{40}Ar/^{39}Ar$ dating of this sample.

margins.

METAMORPHISM AND DEFORMATION

Porphyroblasts in the region and in the contact aureole of the Manzanita pluton contain inclusion trails and porphyroblast-matrix textures that record various stages of development of the S_2 foliation. Collectively, they indicate syndeformational (syn-S_2) growth and retrogression of aureole porphyroblasts.

Kyanite in the Vincent Moore shear zone is interpreted to represent pre-plutonic regional metamorphic conditions. It is lineated and boudinaged parallel to the S_2 foliation and defines the stretching lineation. This indicates that the kyanite formed before or during the development of the regional S_2 foliation. Chloritoid, which is found north of the Manzanita pluton and probably also represents regional metamorphic conditions, originally grew parallel to S_0/S_1 and is folded and boudinaged by F_2 (Brown, 1999). Retrograde chlorite and hematite fill cracks and form wings on chloritoid, indicating syn-S_2 retrogression.

Garnet, present in the southern aureole of the Manzanita pluton, frequently does not contain inclusions or has been cracked so that inclusion geometries are obscure. However, several samples contain garnets with equant opaque inclusions, set in a matrix that has a strong foliation that is defined in part by opaque grains that are intensely flattened in the S_2 foliation. We interpret these garnets to have grown at the beginning of deformation before opaque minerals were deformed. Other garnet samples contain undeformed, equant opaques in the center of the garnets, with stretched opaques near the rims. This indicates that deformation began, or intensified, during growth of the rims of these garnets. Still other samples contain garnet with sigmoidal inclusion geometries, and garnet that both overgrows the S_2 foliation and also deflects it, indicating syn-S_2 growth (Fig. 12A–B; see circles 8 and 9, respectively, on Fig. 2 for sample locations). Many garnets are cracked with retrograde chlorite in the cracks and pressure shadows, which indicates that deformation continued after garnets grew and during cooling and retrogression.

Sillimanite is preserved in a mica pseudomorph in one sample on the southern aureole. The sillimanite fibers near the rim are aligned in S_2, indicating sillimanite growth before or during S_2 development, whereas those in the center are more randomly oriented (Fig. 9). This random orientation in the center may be because the earlier porphyroblast or mica protected the sillimanite from deformation, or because some sillimanite grew after the peak intensity of deformation.

Hornblende, present in the southern aureole, shows the development of subgrains as well as the development of newer, smaller crystals within subhedral porphyroblasts, consistent with subgrain rotation recrystallization. Smaller recrysallized hornblende grains and retrogressed chlorite in the tails of hornblende porphyroblasts are parallel with S_2 (Fig. 11). We interpret these textures to indicate that S_2 deformation occurred at high temperatures (perhaps >500°C) and continued during cooling, although the deformation behavior of amphiboles is not well understood (Passchier and Trouw, 1996).

DEFORMATION AND PLUTONISM

Structural relationships and mineral textures within the granite show that the Manzanita pluton was emplaced during the NW–SE shortening event that produced both top-to-the-north thrust-sense shear zones and the regional NE-striking S_2 foliation. Evidence includes: (1) parallel magmatic and solid state fabrics; (2) dynamic recrystallization of feldspar indicating high-T solid state deformation; (3) dike orientations orthogonal and parallel to the S_2 surface compatible with an S_2 kinematic framework; and (4) variably deformed dikes and veins. Collectively, these relationships indicate the pluton was emplaced during D_2 deformation.

Magmatic and solid state fabrics

One indicator of the magmatic flow fabric is the preferred orientation of igneous minerals, particularly euhedral feldspars (Vernon, 1986). When the magma has less than about 50–70% crystals (critical melt fraction), the magma can flow viscously and the feldspars become aligned by the flow field (van der Molen and Paterson, 1979). As cooling continues, an increasingly strong grain network develops (Miller et al., 1990). If deformation continues, the magmatic fabrics become overprinted by high-T, then lower T solid state fabrics as the pluton cools to ambient conditions (Paterson et al., 1989).

Because of the strong overprint of solid-state deformation, determining the presence and kinematics of magmatic fabrics in the Manzanita pluton is difficult. The fabric present in the Manzanita granite is primarily a solid-state foliation with S-C fabrics, σ-porphyroclasts and mantled porphyroclasts. Moreover, the granite is strongly deformed across its entire exposure, and aplite dike relationships (see below) indicate that deformation continued after cooling of the latest liquids of the pluton. Most feldspar crystals show evidence of dynamic recrystallization at their margins, and many are recrystallized across the entire grain, making it difficult to determine the degree to which the direction of elongation is due to either alignment during magmatic flow or solid state plastic deformation (Paterson et al., 1989). This is further complicated by the prevalent sericitization of feldspars in the area.

Nevertheless, there are indications that the solid state fabric progressively overprinted a parallel magmatic fabric. At the outcrop and microscopic scale, megacrystic K-feldspars show a strong alignment parallel to the C planes of S_2. Many of the K-feldspars, while showing some recrystallization, still preserve crystal faces, and in these cases the long crystal face is subparallel to S_2. Plagioclase grains with both Carlsbad

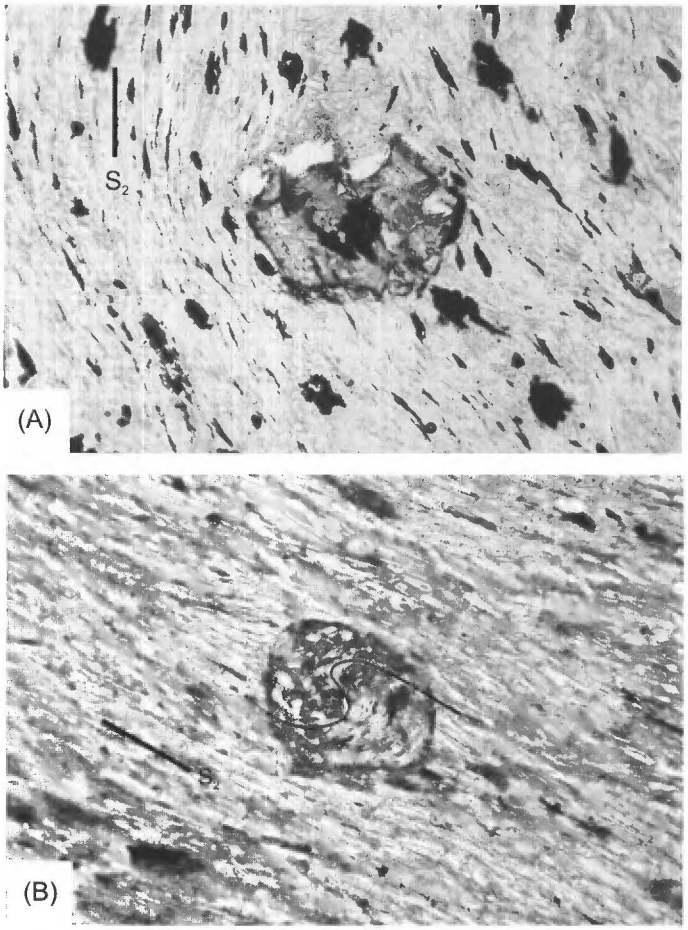


FIGURE 12. Photomicrographs of garnets with syndeformational inclusion geometries. **A**, Garnet has opaque inclusions continuous with S_2 in the matrix, but S_2 is deflected around garnet indicating shortening across S_2 and syndeformational growth. Width of view is 1.35 mm. **B**, Inclusion trails of opaques and micas within the garnets are sigmoidal and are continuous with the S_2 foliation, indicating syndeformational growth. Outline traces inclusion trails. Width of view is 0.52 mm. Sample locations are shown as circles 8 and 9, respectively, on Figure 2.

and albite twins have been observed where the twin boundaries are parallel to the direction of elongation of the grain and the S_2 foliation (Brown, 1999). The presence of the twins indicates that the elongation is probably due to alignment of an igneous crystal during magmatic flow, rather than reorientation of grain shapes in the solid state (Paterson et al., 1989). The magmatic fabric is subparallel to the solid state fabric present in the pluton and continuous with the regional fabric in the country rock.

In the pluton, the S_2 fabric also shows a transition from high-T solid-state flow down through lower temperatures (Fig. 13; see circles 10 and 11, respectively, on Fig. 2 for sample locations). K-feldspars have subgrain development, interlobate grain boundaries formed in response to grain boundary migration recrystallization, and development of regime 3, subgrain rotation recrystallization textures (Hirth and Tullis, 1992), indicating temperatures during deformation of >500°C, depending on strain rate (Tullis, 1983; Simpson, 1985; Tullis and Yund, 1987, 1991; Simpson and Depaor, 1991). Lower-T quartz textures include undulose extinction, core and mantle structures, and textures consistent with subgrain rotation recrystallization and grain boundary migration, representing temperatures during deformation of 250–300°C, depending on strain rate (Gapais and Barbarin, 1986; Simpson and DePaor, 1991; Hirth and Tullis, 1992). Lower-T textures also include feldspar with brittle fracturing and angular grain fragments (250–300°C) and undulose extinction and flame shaped albite lamellae (300–400°C; Tullis and Yund, 1987; Passchier and Truow, 1996). Locally, there is some evidence of annealing in quartz, as shown by small areas of polygonal fabrics accompanied by a larger grain size. Together, the mineral textures indicate that deformation occurred at high and low T, possibly during a continuum of cooling of the pluton down to regional greenschist-grade temperatures.

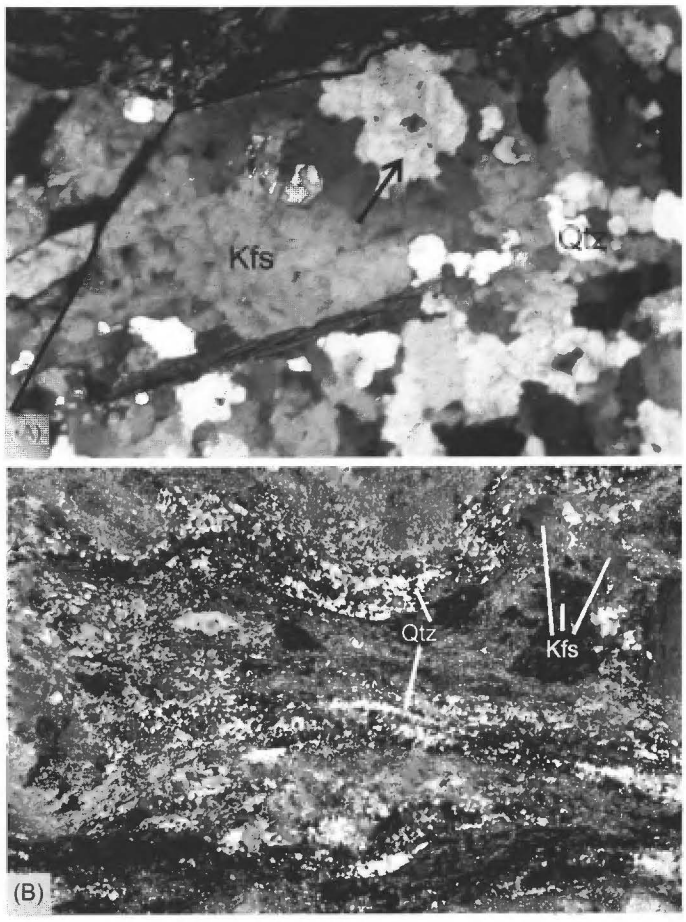


FIGURE 13. **A**, Photomicrograph of Manzanita granite with K-feldspar (Kfs) showing the development of newer, smaller, grains from a larger grain (outlined). Large recrystallized grain with interlobate boundary (arrow), absence of flattened original grains, and a relatively high degree of recrystallization all indicate regime 3 microstructures (T >500°C, depending on strain rate, after Hirth and Tullis, 1992). Clear white grains are quartz (Qtz); cloudy grains are feldspar. Width of view is 1.35 mm. **B**, Photomicrograph of Manzanita granite with cracked K-feldspar (Kfs; upper right) filled with quartz (Qtz; T = 350–500°C) and subgrain rotation recrystallized quartz ribbon textures (T = 250–300°C). Width of view is 17 mm. Sample locations are shown as circles 10 and 11, respectively, on Figure 2.

Dike and vein arrays

Leucocratic granite, aplite, and pegmatite dikes and sills and irregular pods are present within the Manzanita pluton and adjacent greenstone, and are interpreted to represent evolved units of the Manzanita granite. The dikes and sills range from undeformed to strongly deformed. At the outcrop scale the S_2 foliation is not always visible, but even in apparently undeformed dikes and sills the foliation is visible at the microscopic scale, even where the contact is at a high angle to S_2 (Brown, 1999). We interpret these fabrics to mean that deformation continued during cooling of the pluton.

Orientations of poles to dikes and sills show two populations (Brown, 1999). One population of dikes that cross-cut the S_2 foliation (Fig. 14A) has a mean strike and dip of 352, 50E, although there is some degree of scatter in the plot. We interpret these dikes to represent the opening of tensile fractures perpendicular to the stretching lineation (mean plunging 43° towards 141). Therefore, the poles to the cross-cutting dikes (mean of 82, 40S) represent the approximate direction of extension, or Xi, during emplacement of the dikes, compatible with a regionally dominated kinematic framework.

In the second population, sills are concordant with the S_2 foliation (Fig. 14B) with a mean strike and dip of 062, 44S. We interpret these dikes to have been emplaced preferentially along S_2 as a plane of weakness, apparently after substantial cooling of the pluton and significant development of the fabric had occurred. Deformation apparently continued, because there is an S_2 foliation observed in these sills.

In addition, quartz veins injected into country rock both crosscut the S_2 foliation and are folded by F_2 folds, indicating the presence of hydrous fluids during the S_2 foliation development. Collectively, the dike and vein orientations indicate syn-plutonic emplacement as shown in Figure 14.

DISCUSSION

Although any one argument for synkinematic emplacement of the Manzanita pluton might be refuted by another explanation (Brown, 1999), the combined weight of evidence is compelling. The best evidence that pluton emplacement was syn-S_2 and synmetamorphic includes: (1) syndeformational metamorphic porphyroblasts spatially and genetically related to the pluton; (2) high-T (>500°C) shear fabrics in the pluton that are higher temperature than regional metamorphic grade away from the pluton and therefore require extra heat from the pluton; and (3) dike relationships consistent with an S_2 kinematic framework.

Pluton emplacement and cooling are relatively fast, generally <1 m.y. (van der Molen and Paterson, 1979; Paterson and Tobisch, 1992), whereas deformation would have occurred over perhaps 10 m.y. (Hamilton, 1988; Karlstrom and Bowring, 1991; Paterson and Tobisch, 1992). This is consistent with the evidence that the pluton was emplaced during deformation, and that deformation occurred before, during, and after emplacement of the pluton, including during cooling of the most evolved liquids of the pluton as represented by aplite dikes.

The apparent lack of a contact aureole on the north margin could be explained by intense retrogression along the pluton margins. Alternatively, the aureole on the north may have been removed by thrusting. The intense shearing evident across the entire pluton is north verging; if shearing in the Manzanita shear zone on the north margin continued after pluton cooling and after most of the shearing in the Isleta shear zone on the south margin, it could have removed most or all of the north aureole after the pluton had lost most of its thermal budg-

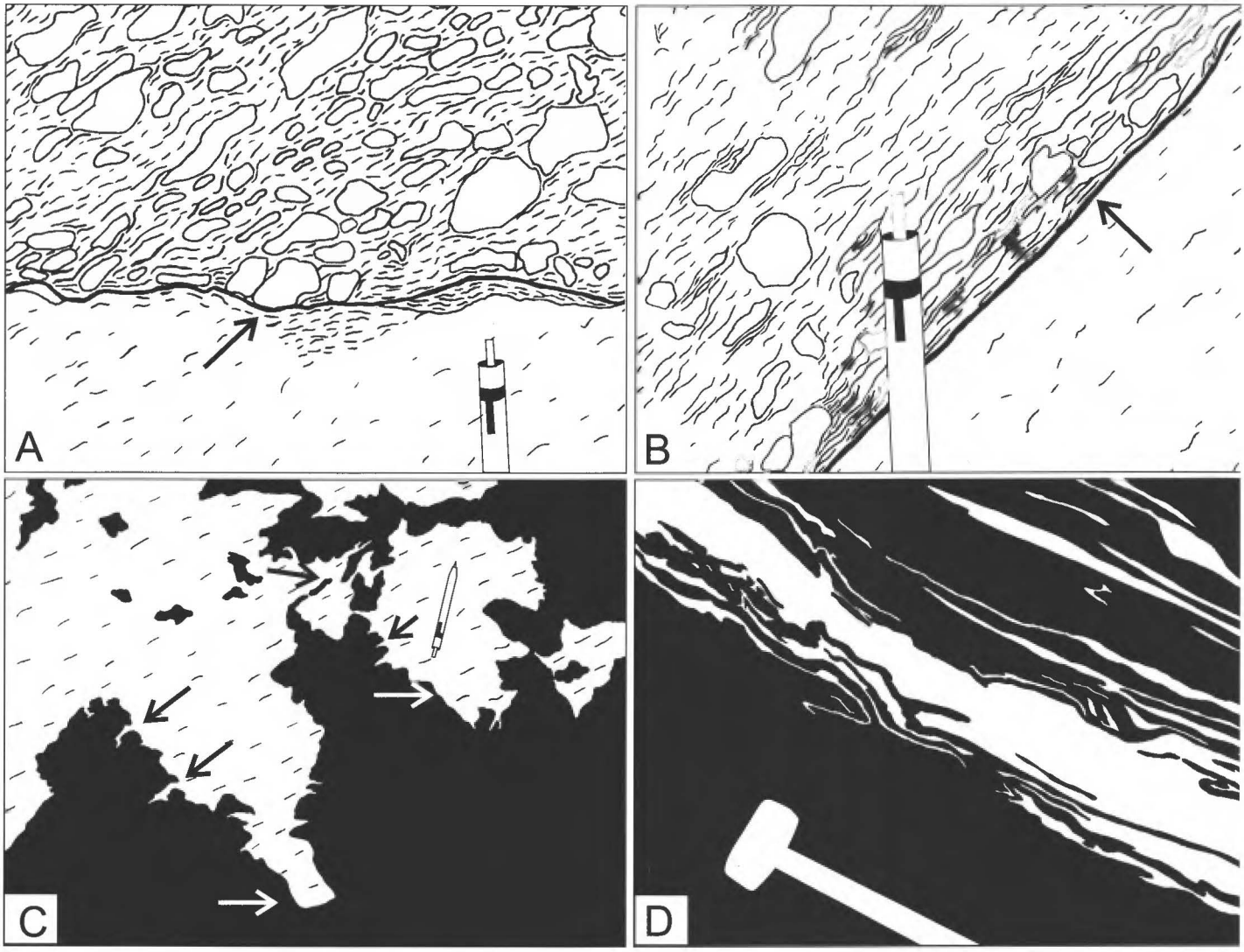


FIGURE 14. Summary of sketches from field photographs of dike, granite, and vein relationships. **A**, Weakly foliatied aplite dike (lower) in contact with granite, looking south. The S_2 foliation is at an angle to the contact, but is deflected somewhat along the contact (arrow), indicating dike emplacement during deformation with deformation continuing after cooling. **B**, Weakly foliated aplite sill (lower right) in contact with granite (arrow), looking south. The contact parallels the S_2 foliation and indicates dike emplacement after foliation development. **C**, Quartz veins (black) in phyllite (white), looking north and down, that both cross-cut (white arrows) and are folded by S_2 (black arrows), indicating the presence of hydrous fluids during S_2 deformation. **D**, Finely interlayered granite (black) and phyllite (white), looking east, which may indicate the presence of granite melt during S_2 deformation. Most of the black (granite) areas also contain fine layers of phyllite that are too small to be shown. Note top-to-the-north (left) shear sense. Form lines in all drawings follow the orientation of S_2.

et. This is consistent with the ubiquitous low-T quartz temperatures in the mylonite zone and with piggyback (foreward) propagation of thrusts (Boyer and Elliot, 1982). Some of this shearing and aureole removal could have occurred at 1.4 Ga as well.

Nature of 1.4-Ga deformation/metamorphism

Evidence for metamorphism and likely deformation occurring at 1.4 Ga is also available. A hornblende date of 1.432 Ga from a sample on the south margin of the pluton suggests temperatures may have been near 500°C at 1.4 Ga. This is compatible with many 1.4-Ga hornblendes in the area (Karlstrom et al., 1997; Marcoline et al., 1999). Hornblende in this area, however, grew during contact metamorphism at 1.65 Ga, and it is difficult to explain the 1.43-Ga hornblende age as simply related to cooling since ca. 1.65 Ga. The thermal effects of pluton emplacement would be short-lived, and the region would presumably return to the relatively cool conditions consistent with the greenschist metamorphic grade. Therefore, we suggest that reheating at 1.4 Ga has caused argon loss and resetting of the K96-1 hornblende rather than simple exhumation of deep crustal rocks at ca. 1.4 Ga.

However, another hornblende dated at 1.67 Ga on the south margin indicates temperatures at 1.4 Ga did not exceed the closure temperature for hornblende for long enough to reset this grain. Farther to the south of the pluton in the Hell Canyon area, the amphibole-bearing samples contain actinolite and little or no hornblende. This indicates that regional metamorphism at 1.4 Ga around 500°C documented by others in the Manzano Mountains farther to the south (Thompson et al., 1996; Marcoline et al., 1999) was lower in temperature going north towards the Manzanita pluton, or was truncated by movement on thrusts in the region. Thus, the peak temperature at 1.4 Ga was likely 400–500°C in the vicinity of the south margin of the Manzanita pluton, with perhaps lower temperatures on the north margin, and duration of heating may have been relatively short.

This degree of heating in and around the Manzanita pluton at 1.4 Ga (400–500°C) caused by regional metamorphism would likely have annealed low-T quartz fabrics. Thus, because annealed textures are found only in isolated areas, we interpret the deformation of quartz at 250–300°C to have occurred at 1.4 Ga as well as at 1.65 Ga. This later deformation apparently reactivated the shear zones that formed initial-

ly at 1.65 Ga, and was probably much less intense than the earlier shearing and thrusting. The area of most intense thrusting is in the mylonite zone on the pluton's north margin where temperatures at 1.4 Ga were probably <400°C and only mild deformation would be required to prevent widespread annealing of the low-T textures.

The S_3 foliation is generally mild to moderate and variably developed to the south of the Manzanita pluton. The rhyolite dike, with a lack of S_2 associated deformation, and alignment of micas along S_3 and the edge crenulated along the F_3 fold axis, cooled through 300°C at 1.428 Ga. The dike could have crystallized much earlier, with the argon clock reset at 1.428 Ga during reheating. This would mean that there was no reactivation of S_2 shear zones at 1.4 Ga. The S_3 fabric, however, is present only locally, and it is difficult to explain the preservation of ubiquitous low-T fabrics throughout the area based on only the D_3 event. Therefore, we suggest that the dike crystallized and cooled at 1.428 Ga shortly after cessation of S_2 associated reactivation, and during the D_3 event.

Summary of events, emplacement model, and P-T-D-t path

A summary of our interpretation of the events is as follows: Prior to 1.65 Ga, regional greenschist metamorphism was occurring at approximately 380–500°C and pressure above 2.5 kbar, as indicated by the presence of kyanite and actinolite + epidote. As the Manzanita pluton was emplaced, it added heat to the crust, producing thermal softening, and deformation (perhaps with decompression) began or intensified. The S_1 and S_2 foliations were formed at this time as part of progressive northwest-verging thrusting. The intense mylonite zone on the north margin of the Manzanita pluton also formed during this thrusting event, probably after significant cooling of the pluton and thrusting on the south margin. Syndeformational contact metamorphic porphyroblasts also grew, including sillimanite, garnet, Fe-rich andalusite + K-feldspar, and hornblende, and indicate the pluton was emplaced at approximately 600–620°C and 2–3 kbar. Deformation continued during and after emplacement and cooling of the pluton, producing ubiquitous retrograde reactions and high-T and low-T ductile textures in feldspars and quartz. The deformation outlasted cooling of the pluton, but was punctuated by heat from the pluton.

At 1.4 Ga, there may have been some regional metamorphism on the southern side of the pluton approaching 500°C, accompanied by renewed thrusting. There may also have been major movement on the Monte Largo thrust to the south (Thompson et al., 1996; Marcoline et al., 1999) because the Priest pluton was emplaced at 4 kbar at 1435 Ma and was brought up to the same crustal level as the Sandia-Manzanita area (2–3 kbar) prior to deposition of the Sandia Formation sandstone in the Pennsylvanian. All deformation associated with S_2 had stopped by 1428 Ma as shown by the rhyolite dike south of the pluton, which has only a mild S_3 foliation.

A schematic model for thrusting and pluton emplacement is shown in Figure 15A. Even in a contractional regime, there are zones of extension as strain is partitioned (Lageson et al., 1994). In a ramp and flat thrust system, there can be passive emplacement of plutons along the ramp (Karlstrom and Williams, 1995). This model is supported by the Coyote and Isleta synclines above the proposed location of the flats and the Hell Canyon anticline above the proposed location of the ramp adjacent to the pluton (Chamberlain, et al., 1997), a geometry typical for thrust systems (Boyer and Elliot, 1982).

We propose an isobaric heating and cooling P-T-D-t path shown in Figure 15B, although there may have been some decompression during pluton emplacement. The rocks started at the surface and were buried to shallow to mid-crustal levels of perhaps 7–15 km, indicated by the presence of early kyanite and pressures >2.5 kbar. During synchronous thrusting and pluton emplacement, the rocks were heated, either isobarically or perhaps with some decompression (with accompanying unroofing), as indicated by andalusite replacing kyanite and peak T and P of 600–620°C and 2–3 kbar (6–9 km) in the pluton aureole. This was apparently followed by isobaric cooling, as indicated by the depth of emplacement of 1.4-Ga magmatic rocks: the rhyolite dike to the south was likely shallow, ~2kbar (hypabyssal textures), and emplacement of

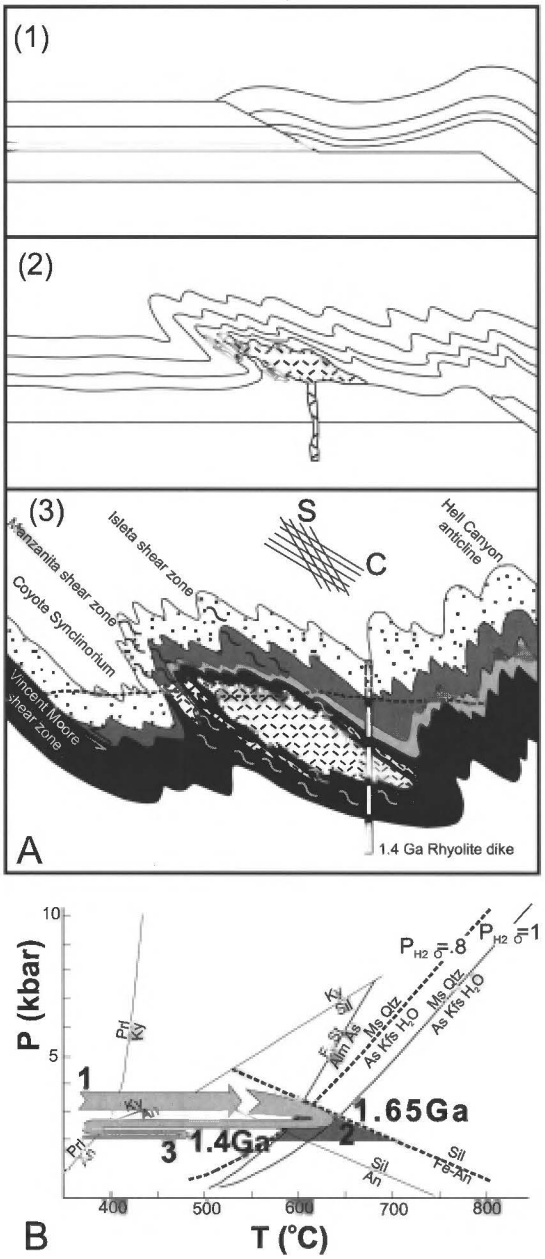


FIGURE 15. **A**, Schematic summary of proposed sequence of events, looking east: (**1**) Thrust belt initiated, with primary controls being brittle faults, with some ductile deformation and beginning of ramp and flat structure. (**2**) At base of ramp, by Manzanita shear zone, room is made by thrusting, and Manzanita pluton (cross hatched area) begins to be emplaced at 1.65 Ga. Ductile deformation continues, thermally enhanced by the pluton. Peak T of 600–620°C is reached. Shearing continues as pluton cools, with strain localized in shear zones. The north aureole is removed by shearing. (**3**) Thrust reactivation and isobaric heating to 400–500°C and cooling at 1.4 Ga. Rhyolite dike south of the Manzanita pluton is emplaced. Vincent Moore shear zone is activated and Sandia pluton emplaced to the north. Simplified cross-section of area of study is shown (see Fig. 2 for location), looking east. S and C shows approximate orientation of S-C fabrics. Rock units are as follows: dotted = sandstone; medium gray = lithic arenite; light gray = phyllite; black = metavolcanics; cross-hatch = Manzanita granite. Heavy dashed line is present day surface. **B**, P-T-D-t diagram showing isobaric heating and cooling paths at 1.65 Ga and 1.4 Ga (light gray areas). Range of probable peak P and T contact metamorphism at 1.65 Ga is shown in medium gray area. Reaction for andalusite = sillimanite is based on increased Fe content; reaction for muscovite + quartz = andalusite + K-feldspar + H_2O is based on lower activity of H_2O (see text; reaction curves are dashed). Reactions are superimposed on aluminum silicate reaction curves (solid lines) after Holdaway (1971) for a Mn, Fe-free system. Numbers correspond to tectonic events shown in A.

the Sandia pluton to the north occurred at 2–3 kbar. Deformation continued after cooling of the pluton, with additional thrusting probably removing the north aureole and placing the granite and rocks from the south aureole against somewhat cooler rocks to the north. Reheating to 400–500°C ca. 1.4 Ga was accompanied by renewed deformation.

ACKNOWLEDGEMENTS

The research for this paper was supported by an NMGS grant (to C. L. Brown) and an NSF grant EAR-9614787 (to K. E. Karlstrom). The authors thank Mark Parchman, Matt Nyman, and Paul Bauer for providing additional samples and the zircon separate; Rick Esser and Lisa Peters from the NMGRL for conducting mineral separations and argon analyses; and Chris Andronicos, Chris Daniel, and Matt Nyman for many useful comments on the manuscript.

REFERENCES

Andronicos, C. L., Karlstrom, K. E., Nyman, E. K. and Timmons, M. T., in preparation, Interactions of metamorphism, deformation, and plutonism in low-pressure, high-temperature metamorphic belts: An example from the Mesoproterozoic Sandia pluton: New Mexico, U.S.A: Journal of Metamorphic Geology.

Apted, M. J. and Liou, J. G., 1983, Phase relations among greenschist, epidote amphibolite, and amphibolite in a basaltic system: American Journal of Science, v. 283-A, p. 328–354.

Barton, M. D. and Hanson, R. B., 1989, Magmatism and the development of low-pressure metamorphic belts: Implications from the western United States and thermal modeling: Geological Society of America Bulletin, v. 101, p. 1051–1065.

Bauer, P. W., Karlstrom, K. E., Bowring, S. A., Smith, A. G. and Goodwin, L. B., 1993, Proterozoic plutonism and regional deformation-new constraints from the southern Manzano Mountains, central New Mexico: New Mexico Geology, v. 15, p. 49–55.

Bauer, P. W. and Williams, M. L., 1994, The age of Proterozoic orogenesis in New Mexico, USA: Precambrian Research, v. 67, p. 349–356.

Bowring, S. A. and Karlstrom, K. E., 1990, Growth, stabilization, and reactivation of Proterozoic lithosphere in the southwestern United States: Geology, v. 18, p. 1203–1206.

Boyer, S. E. and Elliott, D., 1982, Thrust systems: American Association of Petroleum Geologist Bulletin, v. 66, p. 1196–1230.

Brown, C. L., 1999, Synchronous plutonism, metamorphism, and deformation of the 1.65 Ga Manzanita pluton, Manzanita Mountains, New Mexico [M.S. thesis]: Albuquerque, University of New Mexico, in press.

Cavin, W. F., 1985, Precambrian geology of the Manzanita Mountains, New Mexico [M.S. thesis]: Albuquerque, University of New Mexico, 144 p.

Chamberlin, R. M., Karlstrom, K. E., Connell, S. D., Brown, C. L., Nyman, M., Cavin, W. J. and Parchman, M. A., 1997, Geology of the Mount Washington 7.5-minute quadrangle: Bernalillo and Valencia Counties, New Mexico: New Mexico Bureau of Mines and Mineral Resources, Open-file Report DGM 8, scale 1:24,000.

Chatterjee, N. D., 1976, Margarite stability and compatibility relations in the system CaO-Al_2O_2-SiO_2-H_2O as a pressure-temperature indicator: American Mineralogist, v. 61, p. 699–709.

Cosca, M. A. and O'nions, R. K., 1994, A re-examination of the influence of composition on argon retentivity in metamorphic calcic amphiboles: Chemical Geology, v. 112, p. 39–56.

Dahl, P. S., 1996, The effects of composition on retentivity of argon and oxygen in hornblende and related amphiboles: a field-tested empirical model: Geochimica Cosmochimica Acta, v. 60, p. 3687–3700.

Duebendorfer, E. M. and Christensen, C., 1995, Synkinematic(?) intrusion of the "anorogenic" 1425 Ma Beer Bottle Pass pluton, southern Nevada: Tectonics, v. 14, p. 168–184.

Edwards, D. L., 1978, Petrology and structure of Precambrian rocks in the northern North Manzano Mountains and southern Manzanita Mountains, central New Mexico [M.S. thesis]: Albuquerque, University of New Mexico, 87 p.

Gapais, D. and Barbarin, B., 1986, Quartz fabric transition in a cooling syntectonic granite (Hermitage Massif, France): Tectonophysics, v. 125, p. 357–370.

Gonzales, D. A., Karlstrom, K. E. and Siek, G. S., 1996, Syncontractional crustal anatexis and deformation during emplacement of (1435 Ma plutons, western Needle Mountains, Colorado: Journal of Geology, v. 104, p. 215–223.

Grambling, J. A. and Dallmeyer, R. D., 1993, Tectonic evolution of Proterozoic rocks in the Cimarron Mountains, northern New Mexico, USA: Journal of Metamorphic Geology, v. 11, p. 739–756.

Grambling, J. A. and Williams, M., 1985, The effects of Fe^{3+} and Mn^{3+} on aluminum silicate phase relations in north-central New Mexico, U.S.A: Journal of Petrology, v. 26, p. 324–354.

Grambling, J. A., 1988, A summary of Proterozoic metamorphism in northern New Mexico: The regional development of 520C, 4Kbar rocks; *in* Ernst, W. G., ed., Metamorphism and crustal evolution of the western United States: Rubey Volume VII, Prentice Hall, Englewood Cliffs, New Jersey, p. 447–465.

Hamilton, W. B., 1988, Plate tectonics and island arcs: Geological Society of America Bulletin, v. 100, p. 1503–1527.

Harrison, T. M., 1981, Diffusion of $^{40}Ar/^{39}Ar$ in hornblende: Contributions to Mineralogy and Petrology, v. 78, p. 324–331.

Harrison, T. M. and Fitz Gerald J. D., 1986, Exsolution in hornblende and its consequences for $^{40}Ar/^{39}Ar$ age spectra and closure temperature: Geochimica et Cosmochimica Acta, v. 50, p. 247–253.

Heizler, M. T., 1998, Amphibole $^{40}Ar/^{39}Ar$ analyses from the Manzanita Mountains, New Mexico: New Mexico Bureau of Mines and Mineral Resources, Open-file Report 5, p. 1–6.

Heizler M. T. and Harrison, T. M., 1988, Multiple trapped argon isotope components revealed by $^{40}Ar/^{39}Ar$ isochron analysis: Geochimica et Cosmochimica Acta, v. 52, p. 1295–1303.

Hirth, G. and Tullis, J., 1992, Dislocation creep regimes in quartz aggregates: Journal of Structural Geology, v. 14, p. 145–160.

Holdaway, M. J., 1971, Stability of andalusite and the aluminum silicate phase diagram: American Journal of Science, v. 271, p. 97–131.

Holland, T. G. B. and Powell, R., 1990, An enlarged and updated internally consistent thermodynamic dataset with uncertainties and correlations: The system K_2O-Na_2O-CaO-MgO-MnO-FeO-Fe_2O_3-Al_2O_3-TiO_2-SiO_2-C-H_2-O_2: Journal of Metamorphic Geology, v. 8, p. 89–124.

Karlstrom, K. E., Dallmeyer, D. A. and Grambling, J. A., 1997, Mesoproterozoic (1.42–1.35 Ga) regional metamorphism in New Mexico and implications for thermal evolution of lithosphere in the southwestern USA: Evidence from ^{40}Ar-^{39}Ar ages: Journal of Geology, v. 105, p. 205–223.

Karlstrom, K. E. and Bowring, S. A., 1988, Early Proterozoic assembly of tectonostratigraphic terranes in southwestern North America: Journal of Geology, v. 96, p. 561–576.

Karlstrom, K. E. and Bowring, S. A., 1991, Styles and timing of early Proterozoic deformation in Arizona: constraints on tectonic models; *in* Karlstrom, K. E. ed., Proterozoic geology and ore deposits of Arizona: Arizona Geological Society Digest, v. 19, p. 1–10.

Karlstrom, K. E. and Williams, M. L., in press, Heterogeneity of the middle crust: Implications for strength of continental lithosphere: Geology.

Karlstrom, K. E. and Williams, M. L., 1995, The case for simultaneous deformation, metamorphism and plutonism: An example from Proterozoic rocks in central Arizona: Journal of Structural Geology, v. 17, p. 59–81.

Kerrick, D., 1990, The Al_2SiO_5 polymorphs: Reviews in Mineralogy: Mineralogical Society of America, v. 22, 406 p.

Kerrick, D., 1972, Experimental determination of muscovite + quartz stability with $P_{H2O} < P_{total}$: American Journal of Science, v. 272, 946–958.

Kirby, E., Karlstrom, K. E., Andronicos, C. L. and Dallmeyer, R. D., 1995a, Tectonic setting of the Sandia pluton: An orogenic 1.4 Ga granite in New Mexico: Tectonics, v. 14, p. 185–201.

Kirby, E., Karlstrom, K. E. and Andronicos, C. L., 1995b, Structural and thermal setting during emplacement of the Sandia pluton: New Mexico Geological Society, Guidebook 46, p. 219–225.

Krogh, T. E., 1978, Vapour transfer for the dissolution of zircons in a multi-sample capsule, at high pressure; *in* Zartman, R. E., ed., Short papers on the fourth international conference, geochronology, cosmochronology, isotope geology: U.S. Geological Survey, Open-file Report 78-701, p. 233.

Krogh, T. E., 1982, Improved accuracy of U-Pb zircon ages by creation of more concordant systems using air abrasion techniques: Geochimica et Cosmochimica Acta, v. 46, p. 637–649.

Lageson, D. R., Schmitt, J. G. and Burton, B. R., 1994, Upper Cretaceous magmatism and development of a super-critically-tapered thrust wedge in the Sevier orogenic belt of western Montana: Geological Society of America, Abstracts with Programs, p. A-316.

Laird, J. and Albee, A. L., 1981, Pressure, temperature, and time indicators in mafic schist: their application to reconstructing the polymetamorphic history of Vermont: American Journal of Science, v. 281, p. 127–175.

Ludwig, K. R., 1980, Calculation of uncertainties of U-Pb isotope data: Earth and Planetary Science Letters, v. 46, p. 212–220.

Ludwig, K. R., 1985, ISOPLOT200: A plotting and regression program for isotope geochemists, for use with HP series 200 computers: U.S. Geological Survey, Open-file Report 85-513, 102 p.

Marcoline, J., Heizler, M, Goodwin, L. B., Ralser, S. and Clark, J., 1999, Thermal, structural, and petrological evidence for 1400 Ma metamorphism and deformation in central New Mexico: Rocky Mountain Geology, v. 33, in press.

Miller, C. F., Watson, E. B. and Harrison, T. M., 1990, Perspectives on the

source, segregation, and transport of granitoid magmas: Transcripts of the Royal Society of Edinburgh, v. 79, p. 135–156.
Miyashiro, A., 1994, Metamorphic petrology: UCL Press Limited, London, p. 284–285.
Myers, D. A. and McKay, E. F., 1970, Geologic map of the Mount Washington quadrangle, Bernalillo and Valencia Counties, Mexico: U.S. Geological Survey, Geologic Quadrangle Map GQ-886, scale 1:24,000.
Nyman, M. W., Karlstrom, K. E., Kirby, E. and Graubard, C. M., 1994, Mesoproterozoic contractional orogeny in western North America: Evidence from ca. 1.4 Ga plutons: Geology, v. 22, p. 901–904.
Onstott, T. C. and Peacock, M. W., 1987, Argon retentivity of hornblendes: A field experiment in a slowly cooled metamorphic terrane: Geochimica et Cosmochimica Acta, v. 51, p. 2891–2903.
Parchman, M. A., 1981, Precambrian geology of the Hell Canyon area, Manzano Mountains, New Mexico [M.S. thesis]: Albuquerque, University of New Mexico, 108 p.
Passchier, C. W. and Trouw, R. A. J., 1996, Microtectonics: Springer Publishing, New York, 288 p.
Paterson, S. R. and Tobisch, O. T., 1988, Using pluton ages to date regional deformations: Problems with commonly used criteria: Geology, v. 16, p. 1108–1111.
Paterson, S. R. and Tobisch, O. T., 1992, Rates of geological processes in magmatic arcs: Implications for the timing and nature of pluton emplacement and wall rock deformation: Journal of Structural Geology, v. 14, p. 291–300.
Paterson, S. R., Vernon, R. H. and Tobisch, O. T., 1989, A review of criteria for the identification of magmatic and solid state foliations in granitoids: Journal of Structural Geology, v. 11, p. 349–363.
Pedrick, J. N., Karlstrom, K. E. and Bowring, S. A., 1998, Reconciliation of conflicting tectonic models for Proterozoic rocks of northern New Mexico: Journal of Metamorphic Geology, v. 16, p. 687–707.
Ralser, S., Unruh, R. M., Goodwin, L. B., Bauer, P. W., 1997, Geochronologic and microstructural evidence for 1.4 Ga deformation in the southern Manzano Mountains, New Mexico (abs.): New Mexico Geological Society, Proceedings Volume, p. 61.
Read, A. S., Karlstrom, K. E., Grambling, J. A., Bowring, S. A., Heizler, M. and Daniel, C., 1999, A mid-crustal cross section from the Rincon Range, northern New Mexico: Evidence for 1.68 Ga pluton-enhanced tectonism and 1.4 Ga regional metamorphism: Rocky Mountain Geology, v. 33, in press.
Reiche, P., 1949, Geology of the Manzanita and north Manzano Mountains, New Mexico: Geological Society of America Bulletin, v. 60, p. 1183–1212.
Simpson, C., 1985, Deformation of granitic rocks across the brittle-ductile transition: Journal of Structural Geology, v. 7, p. 503–511.
Simpson, C. and DePoar, D., 1991, Deformation and kinematics of high-strain zones: 1991 Annual Geological Society of America Meeting (San Diego), Short Course Notes, 116 p.
Simpson, C. and Schmidt, S. M., 1983, An evaluation of criteria to deduce the sense of movement in sheared rocks: Geological Society of America Bulletin, v. 94, p. 1281–1288.
Spear, F. S., 1993, Metamorphic phase equilibria and pressure-temperature-time paths. Mineralogical Society of America, Washington D.C., 799 p.
Spear, F. S. and Cheney, J. T., 1989, A petrogenetic grid for pelitic schists in the system SiO_2-Al_2O_3-FeO-MgO-K_2O-H_2O): Contributions to Mineralogy and Petrology, v. 101, p. 149–164.
Stacey, J. S. and Kramers, J. D., 1975, Approximation of terrestrial lead isotope evolution by a two-stage model: Earth and Planetary Science Letters, v. 26, p. 207–221.
Thompson, J. B. and Norton, S. A., 1968, Paleozoic regional metamorphism in New England and adjacent areas; *in* Zen, E., White, W. S., Hadley, J. B. and Thompson, J. B., eds., Studies of Appalachian geology: Interscience Publishers, New York, p. 319–328.
Thompson, A. G., Grambling, J. A., Karlstrom, K. E. and Dallmeyer, R. D., 1996, Mesoproterozoic metamorphism and $^{40}Ar/^{39}Ar$ thermal history of the 1.4 Ga Priest Pluton, Manzano Mountains, New Mexico: Journal of Geology, v. 104, p. 583–598.
Tobisch, O. T. and Paterson, S. R., 1988, Analysis and interpretation of composite foliations in areas of progressive deformation: Journal of Structural Geology, v. 10, p. 745–754.
Tullis, J., 1983, Deformation of feldspars; *in* Ribbe, P. H., ed., Feldspar mineralogy: Mineralogical Society of America, Short Course Notes, v. 2, p. 297–323.
Tullis, J. and Yund, R. A., 1991, Diffusion creep in feldspar aggregates: Experimental evidence: Journal of Structural Geology, v. 13, p. 987–1000.
Tullis, J. and Yund, R.A., 1987, Transition from cataclastic flow to dislocation creep of feldspar: mechanisms and microstructures: Geology, v. 15, p. 606–609.
Van der Molen, I. and Paterson, M. S., 1979, Experimental deformation of partially melted granite. Contributions to Mineralogy and Petrology, v. 70, p. 299–318.
Vernon, R. H., 1986, K-feldspar megacrysts in granites-phenocrysts, not porphyroblasts: Earth Science Review, v. 23, p. 1–63.
Villa, I. M., Grobety, B., Kelley, S. P., Trigila, R. and Wieler, R., 1996, Assessing Ar transport paths and mechanisms in the McClure Mountains hornblende: Contributions to Mineralogy and Petrology, v. 126, p. 67–80.
Williams, M. L., 1991, Heterogenous deformation in a ductile fold-thrust belt: The Proterozoic structural history of the Tusas Mountains, New Mexico: Geological Society of America Bulletin, v. 103, p. 171–188.
Williams, M. L., 1994, Sigmoidal inclusion trails, punctuated fabric development and interactions between metamorphism and deformation: Journal of Metamorphic Geology, v. 12, p. 1–21.
Williams, M. L., Karlstrom, K. E., Lanzirotti, A., Read, A. S., Bishop, J. L., Lombardi, C. E., Pedrick, J. N. and Wingsted, M. B, 1999, New Mexico middle crustal cross sections: 1.65 Ga macroscopic geometry, 1.4 Ga thermal structure and continued problems in understanding crustal evolution: Rocky Mountain Geology, v. 33, in press.

APPENDIX—URANIUM-LEAD RELATIONSHIPS FOR ZIRCON SEPARATES FROM SAMPLE NM-91, MANZANITA GRANITE

Sample	Type[2]	WT (mg)	Pb PPM	U PPM	$^{204}Pb/^{206}Pb$[3]	Atomic Ratios[1] $^{206}Pb/^{238}U$	$^{207}Pb/^{235}U$	$^{07}Pb/^{206}Pb$
NM91-4-5	S	0.007*	84.3	616.6	0.0013	0.1196 ± 0.0006	1.632 ± 0.024	0.09901 ± 0.00138
NM91-4-6	S	0.005*	122.4	939.4	0.0001	0.1235 ± 0.0009	1.700 ± 0.017	0.09981 ± 0.00063
NM91-7-1	S-A	0.015*	95.4	516.2	0.0016	0.1649 ± 0.0007	2.297 ± 0.012	0.10101 ± 0.00030
NM91-7-2	S-A	0.01*	95.2	567.1	0.0011	0.1512 ± 0.0006	2.068 ± 0.011	0.09922 ± 0.00032
NM91-7-3	S-A	0.01*	81.5	328.1	0.0013	0.2186 ± 0.0009	3.011 ± 0.017	0.09991 ± 0.00037
NM91-7-4	S-A	0.01*	49.4	299.8	0.0006	0.1567 ± 0.0006	2.169 ± 0.010	0.10038 ± 0.00024
NM91-7-5	S-A	0.01*	75.0	364.1	0.0024	0.1753 ± 0.0007	2.437 ± 0.014	0.10084 ± 0.00043
NM91-7-6	M-A	0.05*	76.7	426.6	0.0010	0.1579 ± 0.0006	2.180 ± 0.009	0.10012 ± 0.00017
NM91-20-1	S-A	0.005	101.2	343.2	0.0043	0.2214 ± 0.0030	3.086 ± 0.048	0.10109 ± 0.00071
NM91-20-2	S-A	0.004	102.7	469.4	0.0018	0.1837 ± 0.0016	2.545 ± 0.025	0.10051 ± 0.00040
NM91-20-3	S-A	0.004	128.7	608.7	0.0012	0.1902 ± 0.0016	2.640 ± 0.024	0.10068 ± 0.00032
NM91-20-6	S-A	0.017	90.8	456.2	0.0006	0.1820 ± 0.0017	2.523 ± 0.029	0.10055 ± 0.00037

[1]Relative to an assumed initial Pb isotopic composition of $^{206}Pb/^{204}Pb$ =16.434 and $^{207}Pb/^{204}Pb$ = 15.392 (Stacey and Kramers, 1975). Uncertainties are at the 95% C.I. (Ludwig, 1980).
[2]S = single-grain analysis, M = multiple-grain analysis, A = air-abraded (Krogh, 1982).
[3]Corrected for mass fractionation of 0.13% ± 0.03% per AMU during mass spectrometery and analytical Pb blanks of 10–20 pg (10^{-12} g).
* Sample weights visually estimated. Consequently U and Pb concentrations are approximate.